



Cite this: *Inorg. Chem. Front.*, 2023, **10**, 5555

## Porous framework materials for stable Zn anodes in aqueous zinc-ion batteries†

Liling Lei, Jiahao Dong, Siwen Ke, Shishan Wu \* and Shuai Yuan \*

Zinc-ion batteries (ZIBs) have attracted widespread research attention because of their safety, cost-effectiveness, and high theoretical capacity; however, challenges related to Zn anodes, such as corrosion in aqueous electrolytes and dendrite growth, impede their practical applications. Metal-organic frameworks (MOFs) and covalent organic frameworks (COFs) have been extensively investigated for stable Zn anodes due to their designable porous structure and tunable surface properties, resulting in substantial advancements. This review provides an overview of the research efforts on MOFs/COFs employed in Zn anodes of ZIBs, including an explanation of the basic concept and existing problems associated with Zn anodes, and a summary of MOF/COF-based materials addressing these challenges. Particular emphasis is placed on establishing the relationship between the MOF/COF structure and their electrochemical performance in ZIBs. Finally, challenges and perspectives with MOF/COF-based materials for future aqueous zinc ion energy storage equipment are put forward. Overall, this review aims to guide the synthesis of suitable MOF/COF-based materials to improve the stability of the Zn anode for ZIBs.

Received 3rd July 2023,  
Accepted 27th July 2023  
DOI: 10.1039/d3qi01222k  
[rsc.li/frontiers-inorganic](http://rsc.li/frontiers-inorganic)

### 1. Introduction

With the advancement of society and technology, the increasing energy demand necessitates the exploration of sustainable options. While renewable sources such as wind, solar, and hydropower have gained popularity, their intermittent nature

and susceptibility to time, season, and climate pose challenges in their widespread application. Rechargeable batteries offer a promising solution to ensure stable energy supply, with lithium batteries being the most prevalent due to their high energy density.<sup>1–4</sup> However, Li batteries have certain limitations including high costs associated with lithium metal, and flammability concerns with organic electrolytes.<sup>5</sup> As an alternative to Li batteries, zinc-ion batteries (ZIBs) have gained attention with the merits of low price of Zn metal, safety in aqueous electrolytes, high theoretical capacity (volume capacity of 5855 mA h cm<sup>−3</sup> and weight capacity of 820 mA h g<sup>−1</sup>), and environmental benignity.<sup>6,7</sup> However, dendrite growth, corrosion and the hydrogen evolution reaction

State Key Laboratory of Coordination Chemistry, Key Laboratory of Mesoscopic Chemistry of MOE, School of Chemistry and Chemical Engineering, Nanjing University, Nanjing 210023, P. R. China. E-mail: syuan@nju.edu.cn, shishanwu@nju.edu.cn

† Electronic supplementary information (ESI) available. See DOI: <https://doi.org/10.1039/d3qi01222k>



Liling Lei received her BS degree and MS degree from Zhengzhou University of Light Industry, China, in 2017 and 2020, respectively. She is now a Ph.D. candidate working jointly in Prof. Shuai Yuan's group and Prof. Shishan Wu's group. Her research mainly focuses on the design and synthesis of MOFs for energy storage applications.

Liling Lei



Jiahao Dong

Jiahao Dong received his B.Eng. degree from China University of Petroleum, Beijing, in 2021. He is now an M.S. student in Prof. Shuai Yuan's group. His research mainly focuses on the synthesis and design of MOFs for biomimetic catalysis.

(HER) occurring at the Zn anode need to be solved for the practical application of ZIBs. The exploration of novel materials, such as metal-organic frameworks (MOFs) and covalent organic frameworks (COFs), presents promising opportunities to address the challenges and achieve high-performance ZIBs.

MOFs/COFs are crystalline porous materials with designable structures, high specific surface areas, and tunable surface properties, and have shown potential in various applications, including gas storage, catalysis, sensing, and energy storage.<sup>8,9</sup> MOFs/COFs are particularly attractive for addressing challenges in aqueous ZIBs. The inherent pores of MOFs/COFs facilitate easy diffusion of  $Zn^{2+}$  ions, while their periodic crystalline structure and ordered channels promote a homogeneous  $Zn^{2+}$  flux. Stable MOFs/COFs separated the Zn anode and the electrolyte achieving the purpose of preventing corrosion, dendrite growth and the HER. Taking advantage of the versatility of MOFs/COFs, they have been applied as Zn anode materials, protective layers of anodes, separators, solid-state electrolytes, and electrolyte additives in ZIBs.

The structures and properties of MOFs/COFs play a crucial role in determining the performance of Zn anodes in batteries. Specifically, the pore sizes, surface area, stability, conductivity and morphology of MOFs/COFs can influence the accessibility of  $Zn^{2+}$  ions to the anode surface and electron transfer, thus controlling the overall performance of the Zn anode. Understanding the correlation between the MOF/COF structures and Zn anode protection function is essential for designing high-performance anodes in ZIBs. Although the applications of MOFs in ZIBs have been comprehensively summarized in several reviews,<sup>10–12</sup> these reviews focus more on the performances of ZIBs. However, the intrinsic structures of MOFs and their relationship to the performance of ZIBs were overlooked. This review will not only summarize the recent research on solving Zn anode issues using MOF/COF-based materials, but also analyze the effect of the MOF/COF structure on their electrochemical performance in ZIBs. In addition, this review will present the current research directions and

future perspectives in the design and synthesis of MOFs/COFs for advancing Zn metal anodes and aqueous ZIBs. We expect that this review will assist the rational design and synthesis of MOF/COF-based materials for aqueous zinc ion energy storage devices.

## 2. Basic concepts

### 2.1 Fundamentals of ZIBs

ZIBs are assembled with Zn metal anodes, cathodes (V oxide, Mn oxide, Prussian blue analogues, quinone, organic cathodes), electrolytes, and separators.  $Zn^{2+}$  ions shuttle between the cathode and the Zn anode during charging/discharging cycles. During charging, the Zn anode loses electrons to generate  $Zn^{2+}$  ions that travel through the electrolyte and insert into the cathode (Fig. 1a) eqn (1).<sup>13</sup>  $Zn^{2+}/H^+$  co-insertion occurs in the  $MnO_2$  cathode. This process is depicted by the following eqn (2) and (3):<sup>14</sup>

Anode:



Cathode:



The main reactions occurring on the Zn anode of ZIBs are Zn plating and stripping. The stability of the Zn anode is hindered by dendrite formation, which punctures the separator and induces short circuits.<sup>15–18</sup> In the initial plating process,  $Zn^{2+}$  near the electrode surface is preferentially reduced and inclined to form small protuberances on the Zn foil. During further plating, the protuberances attract the deposition of more  $Zn^{2+}$  as a result of the “tip effect”. After multiple cycles, dendrites may grow large enough to cause short circuits (Fig. 1b).<sup>19</sup> The uneven electric field distribution and unconstrained 2D diffusion of  $Zn^{2+}$  on the Zn surface cause dendrite formation and reduce the battery life.<sup>20</sup>



Prof. Shishan Wu received his Ph.D. under the supervision of Prof. Xi Xu at Sichuan University in 2000. Since 2001, he has been a professor in Nanjing University. His research mainly focuses on the synthesis and application of graphene composite materials and topological polymers, and energy storage materials.

Shishan Wu



Shuai Yuan

Prof. Shuai Yuan received his Ph.D. in chemistry in 2018 from Texas A&M University under the supervision of Prof. Hong-Cai Zhou. He then moved to MIT for postdoctoral research, where he explored the application of MOFs for electrocatalysis. In 2021, he joined Nanjing University as a professor of chemistry. His research is focused on the design of three-dimensional synergistic catalytic sites using multi-component MOFs.

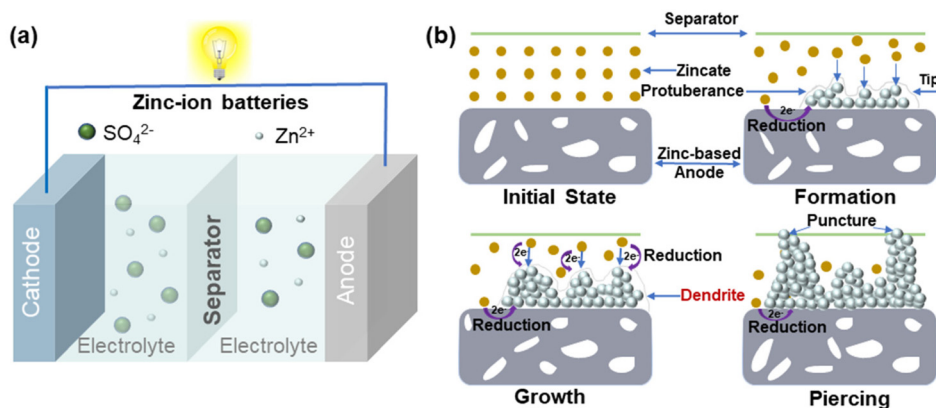
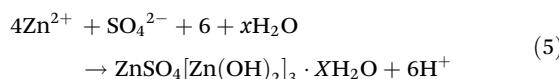


Fig. 1 (a) Schematics of the work mechanism for the aqueous ZIBs and (b) the evolution process on the Zn anode. Reproduced from ref. 19 with permission from John Wiley & Sons, copyright 2018.

Side reactions may happen on the Zn anode by reacting with the electrolytes causing corrosion. For example, Zn metal undergoes slow corrosion in mildly acidic  $ZnSO_4$  aqueous electrolytes (eqn (4) and (5)). Anode corrosion can lead to irreversible consumption of Zn and the formation of inert by-products such as  $Zn_4SO_4(OH)_6 \cdot xH_2O$ .<sup>21</sup> These by-products are formed at the expense of electrolytes and active  $Zn^{2+}$  ions, which decrease the coulombic efficiency (CE) of the Zn anode.<sup>22</sup> Furthermore, the inert by-products on the electrode hinder ion transportation and reduce the reversibility of the Zn anode.



In addition to Zn corrosion, the HER may also happen during the electrodeposition of the Zn anode, where electrons from the external circuit reduce both  $Zn^{2+}$  and  $H^+$ .<sup>23,24</sup> The  $H_2$  produced from corrosion and the HER can increase the pressure of the sealed battery, which poses a safety hazard. Additionally, the process of the HER is unavoidably impacted by competitive Zn plating, reducing CE and leading to local pH instability due to the  $OH^-$  concentration increase.<sup>17</sup> The high concentration of  $OH^-$  ions can in turn promote the formation of inert by-products on the Zn anode.<sup>25</sup>

In general, dendrite formation, corrosion and the HER are closely related: the formation of dendrites increases the surface roughness of the Zn anode, thus accelerating corrosion and the HER. The HER causes the increase of  $OH^-$  and forms inert by-products on the Zn anode surface.<sup>26</sup> This leads to an uneven surface and electric field distribution, further promoting the formation of dendrites. Consequently, the preparation and mechanism of high-performance reversible Zn anodes is a research hotspot in ZIBs.<sup>27</sup> To address the challenges of stable Zn anodes, many materials have been explored. Among them, MOFs and COFs have demonstrated promising potential in addressing the challenges associated with the Zn metal anode.

## 2.2 Structures of MOFs and COFs

MOFs are constructed by combining metals or metal clusters, known as secondary building units (SBUs), with organic linkers, which are often carboxylic acids or nitrogen-containing ligands. The diverse crystal structures of MOFs provide a wide range of functions and properties. The most commonly used MOFs in ZIBs are UiO-66, ZIF-8, and HKUST-1 due to their uniform porosity, high surface area and facile synthesis. UiO-66 is constructed from  $Zr^{4+}$  and a linear dicarboxylate linker BDC (1,4-benzenedicarboxylate).<sup>28</sup>  $Zr^{4+}$  is assembled into a  $Zr_6O_4(OH)_4$  SBU, which is further bridged by 12 BDC linkers into a 3D framework structure. Each unit cell is composed of one octahedral central cage (8 Å) and eight tetrahedral corner cages (6 Å, Fig. 2a). ZIF-8, as a representative example of zeolitic imidazolate frameworks (ZIFs), is composed of  $Zn^{2+}$  ions connected to methylimidazole (mlm) ligands, forming a truncated octahedral cage with a diameter of ~12 Å (Fig. 2b).<sup>29</sup> Within HKUST-1,  $Cu^{2+}$  ions form dimers, with each copper atom being coordinated by four oxygen atoms from BTC (1,3,5-benzenetricarboxylate) linkers (Fig. 2c). It is composed of small octahedral cages (5 Å) and a large truncated octahedral cage (~14 Å).<sup>30</sup> The combination of different SBUs and linkers gives rise to a variety of frameworks with predictable structures, controllable pore sizes and functionalities.

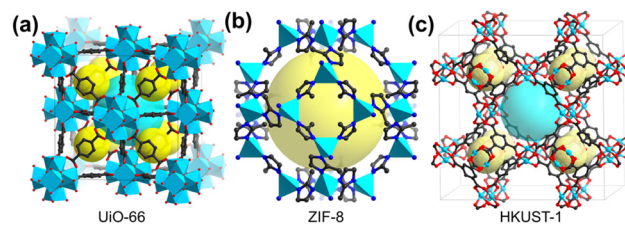


Fig. 2 Crystal structures of (a) UiO-66, reproduced from ref. 28 with permission from American Chemical Society, copyright 2008. (b) ZIF-8, reproduced from ref. 29 with permission from Proceedings of the National Academy of Sciences of the United States of America, copyright 2006. (c) HKUST-1, reproduced from ref. 30 with permission from American Association for the Advancement of Science, copyright 1999.

for targeted applications. This predictive capability facilitates the rational design of novel kinds of MOFs with desired functionalities. Currently, more than 90 000 MOFs have been synthesized, with an additional 500 000 predicted structures, and this number is expected to expand further each year as research in the field continues to advance.

Similar to MOFs, COFs are also porous crystalline materials with large specific surface areas and designable structures, and have diverse applications ranging from gas storage and separation to catalysis, energy storage, and electronics.<sup>31</sup> COFs are pure organic materials formed by linking multifunctional monomers through covalent bonds.<sup>32–34</sup> Over 500 kinds of COF structures featuring various linkages, including boronate ester, imine, triazine, hydrazone, azine, and alkene, have been designed and synthesized (Fig. 3a).<sup>35</sup> Most COFs have 2D layered structures which are stacked *via* weak interactions (e.g., hydrogen bonding and  $\pi$ - $\pi$  stacking interactions) to form 1D channels (Fig. 3b). The robust covalent bonds endow COFs with higher chemical stability compared to MOFs. However, the lower reversibility associated with covalent bond formation presents a challenge in obtaining highly crystalline COF products. This leads to relatively lower structural diversity when compared to MOFs.

### 2.3 Properties of MOFs/COFs

MOFs and COFs are promising materials for ZIBs because of their intrinsic properties such as a large surface area, high porosity, tunable surface functional groups, and controllable morphology. The well-ordered channels promote a homogeneous  $Zn^{2+}$  flux, resulting in uniform Zn nucleation and deposition on the anode surface. Furthermore, taking advantage of their high tunability, a wide range of functional groups (such as  $-SO_3H$ ,  $-COOH$ , and  $C=O$ ) can be incorporated into MOFs/COFs as zincophilic sites to induce uniform Zn deposition. The large surface area of MOFs/COFs allows for a higher number of zincophilic active sites inducing uniform  $Zn^{2+}$  deposition. For electrically insulating but ionic conduction

tive MOFs/COFs, Zn can be deposited under the coating layer, which promotes long-term cycling stability. By separating the Zn anode and electrolytes with MOFs and COFs, corrosion and the HER can be restricted. Some MOFs/COFs exhibit inherent redox activity, allowing them to store and release charge *via* structural redox reactions. Herein, we discuss the properties of MOFs and their impact on the Zn anode performance in aqueous ZIBs.

**2.3.1. High porosity.** MOFs/COFs are famous for their extraordinary porosity and high surface area.<sup>36</sup> The pore size and surface area of MOFs can be precisely adjusted by selecting appropriate linkers and metal nodes, while the porosity of COFs is determined by the monomers. Isoreticular expansion is an effective method to adjust the porosity of MOFs/COFs. Isoreticular MOFs/COFs, defined as frameworks with the same structural topology, are formed by using a library of related organic linkers with different lengths and functionalities. The precise control of the pore size and chemical environment in MOFs/COFs enables the independent investigation of structural and chemical factors that influence electrochemical processes. For example, the pore apertures of MOFs/COFs used in ZIBs are larger than the diameter of  $Zn^{2+}$  (1.48 Å), which allows  $Zn^{2+}$  to pass through. Increasing the BET surface area and pore size of MOFs/COFs can facilitate the even distribution of electric fields, mitigate local current density, and enhance  $Zn^{2+}$  flux, thereby accelerating Zn deposition.<sup>37</sup>

**2.3.2. Tunable surface functional groups.** The functionalization of organic ligands can modulate the electronic state and hydrophilicity of MOFs/COFs, thereby affecting the Zn deposition behaviors. MOFs/COFs can be modified by various electronegative atoms (such as F, P, S, and N) or polar functional groups ( $-COOH$ ,  $-CH_3$ ,  $-SO_3H$ ,  $-NH_2$ ,  $-CF_3$ ,  $-PO_3H$ , and  $-OH$ ) to achieve predictable properties. These modifications create active sites that interact with  $Zn^{2+}$ , resulting in a preferred orientation of Zn deposition on the lower surface energy (002) planes.<sup>38</sup> This ordered Zn deposition helps to prevent short circuits caused by dendrite growth and separator penetration during the plating and stripping processes. Moreover, the zincophilic layer regulates the electrolyte flux on the Zn anode while blocking the movement of  $SO_4^{2-}$  ions, thereby reducing the  $Zn^{2+}$  transfer resistance and improving the  $Zn^{2+}$  transference number.<sup>39</sup> Overall, these modifications optimize the performance of the Zn anode and enhance battery efficiency.

**2.3.3. Controllable morphology.** Precisely controlling the morphology of MOFs/COFs is significant for their applications in Zn anodes. The morphology of MOFs/COFs can be classified into 0D nanoparticles, 1D nanofibers/nanorods, 2D nanoplates/films, and 3D monoliths/foams.<sup>40</sup> Among these morphologies, 2D MOF/COF nanoplates/films are preferred when applied as protective coating layers due to their close adherence to the Zn surface.<sup>41,42</sup> They can prevent electrolyte permeation and inhibit dendritic growth.

**2.3.4. Stability.** The stability and conductivity of MOFs/COFs need to be considered when applied in aqueous ZIBs. The chemical stability of MOFs/COFs refers to their ability to

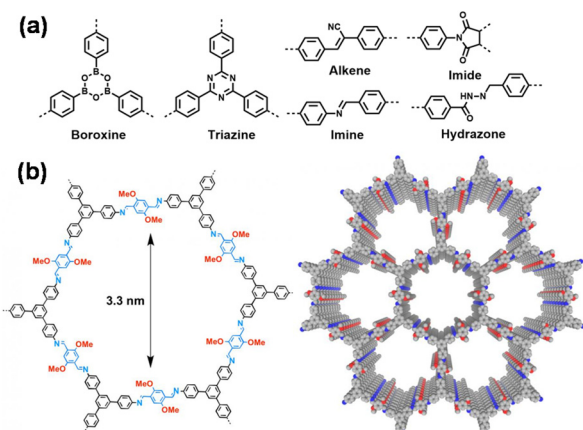


Fig. 3 (a) Various dynamic covalent bonds explored for the synthesis of COFs. (b) Structure of a representative COF. Reproduced from ref. 35 with permission from John Wiley & Sons, copyright 2021.

maintain their crystalline structure in various environments. The thermodynamic stability of MOFs/COFs is primarily attributed to the strength of the coordination and covalent bonds. Therefore, the stronger the coordination and covalent bonds, the more stable the skeleton formed. To achieve high stability for MOFs/COFs, Pearson's hard and soft acids and bases (HSAB) principle and the dynamic covalent chemistry (DCC) principle are usually employed. For instance, stable MOFs have been prepared by assembling soft bases (such as imidazolate, pyrazolate, triazolate and tetrazolate ligands) with soft divalent metal ions (such as  $Zn^{2+}$ ,  $Cu^{2+}$ ,  $Ni^{2+}$ , etc.) or hard bases (such as carboxylate ligands) with high-valent metal ions (such as  $Cr^{3+}$ ,  $Al^{3+}$ ,  $Fe^{3+}$ ,  $Zr^{4+}$  and  $Ti^{4+}$ ), according to the HSAB principle.<sup>43</sup> The stable pH window of MOFs is also dictated by the  $pK_a$  of the ligands: azolate-based MOFs are generally more resistant to alkaline conditions while carboxylate-based MOFs are more stable in acids. It is generally believed that the stability of COFs with robust covalent bonds is higher than that of MOFs with dynamic coordination bonds. For example, COFs with imine bonds are stable in a wide pH range (0–14).<sup>44</sup>

In practice, MOFs and COFs need to be stable in mildly acidic aqueous  $Zn^{2+}$  electrolytes ( $pH = 3.6$ –6.0). Although some MOFs with low-valent metals and carboxylate ligands (such as MOF-5) have been occasionally applied in ZIBs, they tend to decompose in water and aqueous electrolytes. Therefore, the observed electrochemical performance may not be attributed to the intrinsic properties of MOFs. In addition, some research results indicate that ZIF-8 has limited stability under mildly acidic conditions, although ZIF-8 has been commonly applied in ZIBs.<sup>45,46</sup>

**2.3.5. Conductivity.** Most MOFs and COFs are electrical insulators with a conductivity of  $10^{-10}$  S cm<sup>-1</sup> or lower. However, their porous structure allows the transport of  $Zn^{2+}$  through their pores, resulting in good ionic conductivity.<sup>47</sup> These MOFs/COFs with low electrical conductivity but high ionic conductivity are suitable protective layers of Zn anodes, which allows Zn deposition on the Zn surface under the MOF/COF layer. Efforts have been made to improve the electronic conductivity of MOFs/COFs by extending the  $\pi$ -d or  $\pi$ - $\pi$  conjugation of the framework and creating electron transfer pathways. These MOFs/COFs with both electrical and ionic conductivity can be applied as anode materials.<sup>48</sup>

### 3. MOFs/COFs for stable Zn anodes

Currently, a large amount of literature has been reported on improving the cycling stability of Zn anodes,<sup>49–51</sup> for example, through electrolyte engineering,<sup>20,52–54</sup> constructing the Zn anode protective coating,<sup>55–58</sup> designing the anode host structure,<sup>59,60</sup> optimizing separators,<sup>61–63</sup> and exploiting Zn-free anodes.<sup>6,48,64</sup> Specifically, MOFs/COFs have been applied as protective coating layers or Zn hosts of anodes, separators, solid-state electrolytes, and electrolyte additives in ZIBs. Conductive MOFs/COFs have also been directly applied as anode materials to address issues in Zn anodes (Fig. 4).

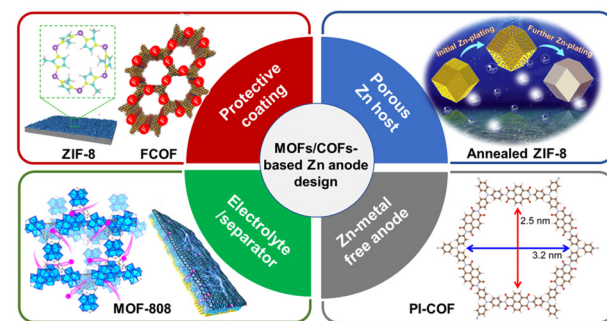


Fig. 4 Roles of MOF/COF-based materials applied for Zn anode modification in aqueous zinc ion energy storage.

Although MOF/COF-derived materials (such as porous carbons and metal oxides) have been intensively reported as effective materials for improving the stability of Zn anodes in ZIBs, these materials lose the structural order of crystalline MOFs/COFs, making it difficult to define structure–function relationships. Therefore, this review focuses on the MOFs/COFs with well-defined structures for ZIBs.

#### 3.1 MOFs/COFs as protective layers

MOFs can act as protective coatings to prevent dendrite formation, corrosion, and the HER on Zn anodes. For example, the stable Zr-MOF (UiO-66) serves as a robust protective layer for Zn anode coating, facilitating dendrite-free Zn deposition (Fig. 5a). Liu *et al.*<sup>65</sup> utilized UiO-66 to enhance the nano-wetting effect of aqueous electrolytes on the Zn anode, building a zincophilic interface. The hydrophilic UiO-66 exhibits a wetting effect and reduces charge-transfer resistance (Fig. 5b and c). The UiO-66 particle-protected layer immersed in the electrolyte can adjust homogeneous  $Zn^{2+}$  ion deposition. This leads to dendrite-free Zn plating/stripping possesses, resulting in stable cycles of the Zn anode for up to 500 cycles (Fig. 5d). In addition, introducing defects (such as oxygen vacancies) in UiO-66 can improve the  $Zn^{2+}$  transference number and ionic conductivity compared to that of defect-free UiO-66. This improvement occurs due to the fixation of anions to the electropositive oxygen vacancies through Lewis acid-base reactions. Based on this idea, Xu *et al.*<sup>66</sup> designed a defect-rich MOF (D-UiO-66) as a quasi-solid electrode/electrolyte interlayer on the Zn anode, which is filled with two types of Zn salt electrolytes as a  $Zn^{2+}$  reservoir. Additionally, the MOF channels were modified with anionic functional groups (such as  $-SO_3^-$ ), which can enhance cation diffusion within the pores. The Zn anode demonstrated stable Zn plating and stripping performance over a period of 1800 h at a current density of 1 mA h cm<sup>-2</sup> (Fig. 5e). The CE achieved during the extended cycling period was 99.8%, demonstrating excellent performance and stability.

To increase the hydrophilicity and ionic conductivity of UiO-66, Xin *et al.*<sup>67</sup> developed a  $-COOH$  functionalized MOF (UiO-66-(COOH)<sub>2</sub>), which serves as an ion conductive interlayer to hinder the HER and achieve a dendrite-free Zn anode

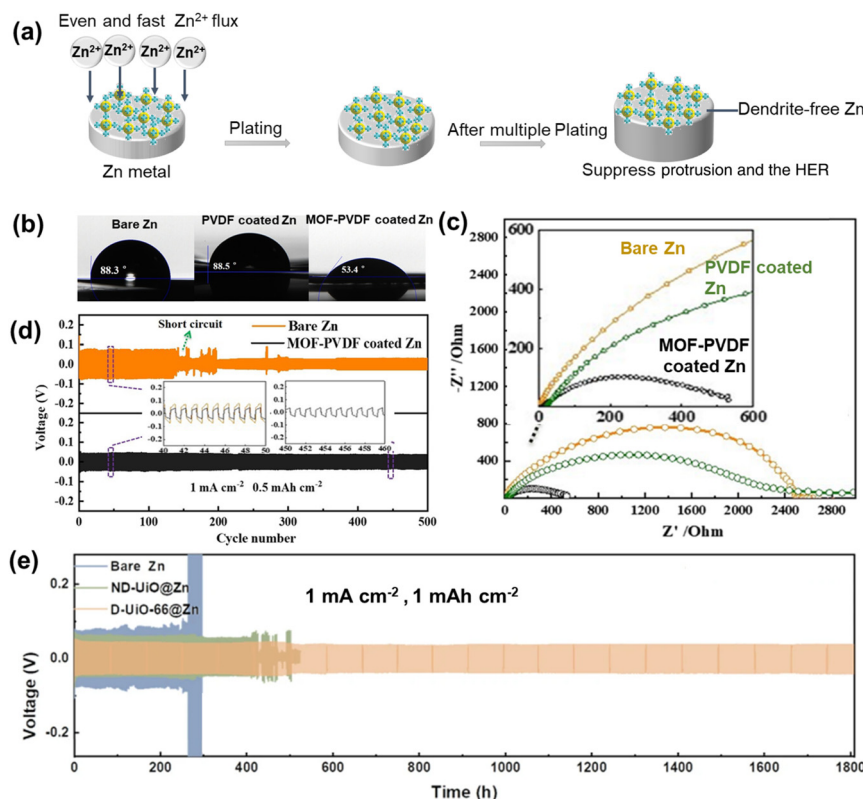


**Fig. 5** (a) Schematic of  $Ui\text{O}-66$  inducing dendrite-free  $Zn$  deposition. (b) Contact angles of electrolyte on different anodes. (c) EIS of  $Zn$ -symmetric cells with different anodes. (d) Voltage profiles of MOF-PVDF coated  $Zn$  in symmetric cells. Reproduced from ref. 65 with permission from American Chemical Society, copyright 2019. (e)  $Zn$  plating/stripping in a symmetric cell based  $ND\text{-}Ui\text{O}@Zn$ ,  $D\text{-}ND\text{-}Ui\text{O}@Zn$  and bare  $Zn$ . Reproduced from ref. 66 with permission from Springer Nature, copyright 2023.

(Fig. 6a). The  $-COOH$  groups promote hydrophilicity and increase ionic conductivity, facilitating the homogeneous deposition of  $Zn^{2+}$  on  $Ui\text{O}-66\text{-}(COOH)_2@Zn$  (Fig. 6b). The  $Zn$  anode protected by  $Ui\text{O}-66\text{-}(COOH)_2$  can be operated for about 2800 h at 2  $mA\ cm^{-2}$  (Fig. 6c) in a symmetric cell. Similarly, Kim *et al.*<sup>68</sup> employed the Zr-MOF ( $Ui\text{O}-66\text{-}(COOH)_2$ ) as a  $Zn$  anode protective layer. PVDF-hexafluoropropylene (PVDF-HFP) was used as a binder additive to suppress dendrite growth, which exhibited higher ionic conductivity and binding affinity compared to PVDF. The stable and porous  $Ui\text{O}-66\text{-}(COOH)_2$  acts as a sieve, permitting  $Zn^{2+}$  ions to be deposited on the  $Zn$  anode evenly, resulting in a dendrite-free surface (Fig. 6d).  $Ui\text{O}-66\text{-}(COOH)_2$  contains  $-COOH$ , which makes it a hydrophilic MOF, facilitating convenient ion transport. The assembled symmetric cells exhibited stable cycle for 200 h at 10  $mA\ cm^{-2}$  (Fig. 6e).

Recently, Zhang *et al.*<sup>69</sup> reported EDTA grafting to Zr-based MOF-808 (MOF-E) as a bifunctionally anodic interlayer with uniform desolvation sites and fast ionic transport channels to stabilize the  $Zn$  anode. EDTA as ion-trapped tentacles coordinate with  $Zn^{2+}$  to quicken the desolvation and ionic transport. MOF-E effectively inhibits side reactions and promotes  $Zn^{2+}$  deposition oriented along the (002) plane (Fig. 7a-c). The MOF-E@Zn symmetric cells demonstrated stable operation for 900 h at a current density of 2  $mA\ cm^{-2}$  (Fig. 7d).

To investigate the effect of morphology on the  $Zn$  anode, our group<sup>41</sup> synthesized two Zr-based MOFs, namely  $Ui\text{O}-67\text{-}3D$  and  $Ui\text{O}-67\text{-}2D$ . Research indicates that  $Ui\text{O}-67\text{-}2D$ , a 2D nanosheet MOF, exhibits excellent film-forming ability and can tightly coat the  $Zn$  anode to effectively prevent dendrite formation and the HER. When used as a protective layer,  $Ui\text{O}-67\text{-}2D$  outperforms  $Ui\text{O}-67\text{-}3D$  and bare  $Zn$  in terms of dendrite suppression and HER inhibition (Fig. 8a). Further mechanism analysis revealed that  $Zr\text{-OH}/H_2O$  provides strong  $Zn$  binding sites for  $Zn$  deposition to be initiated. High  $Zr\text{-OH}/H_2O$  concentration for  $Ui\text{O}-67\text{-}2D$  provides more zincophilic sites, facilitating a dendrite-free  $Zn$  anode during cycling. The assembled symmetric cell based on  $Ui\text{O}-67\text{-}2D$  can operate for over 800 h at 0.5  $mA\ cm^{-2}$  (Fig. 8b).

Different from Zr-MOF, N species contained in ZIF can improve hydrophilicity, ensuring uniform  $Zn$  deposition and forming a dendrite-free  $Zn$  anode. Yang *et al.*<sup>70</sup> investigated the use of MOF (ZIF-7) to create a hydrophobic layer that helps maintain a saturated electrolyte interphase. The ZIF-7 layer prevents direct contact between the aqueous solution and the  $Zn$  anode, thereby reducing corrosion caused by the electrolyte. Additionally, the tight contact between ZIF-7 and  $Zn$  enables the exclusion of large charged ion complexes (Fig. 9a). Raman spectroscopy provided evidence of the removal of  $H_2O$

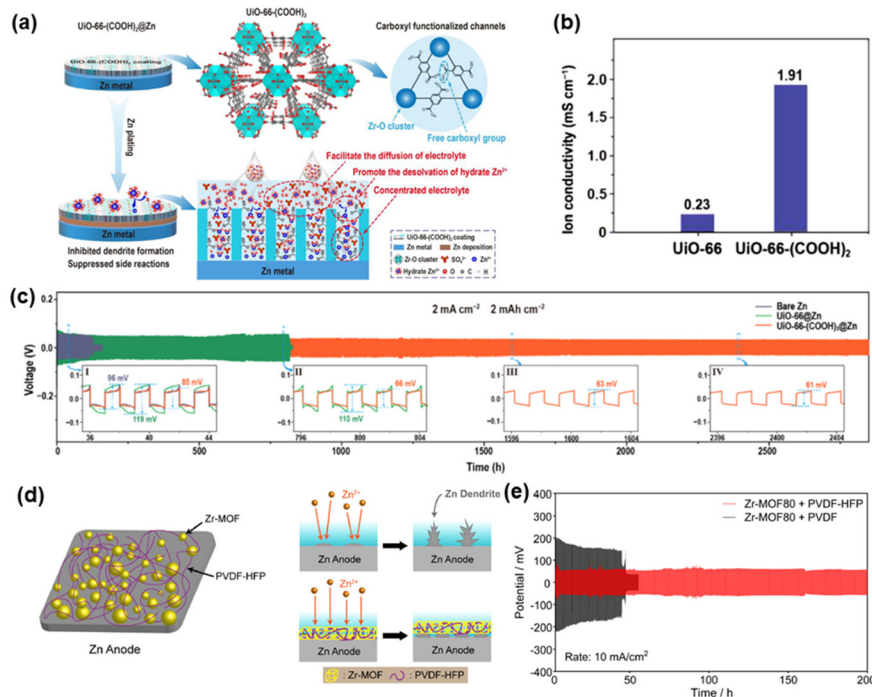


**Fig. 6** (a) Schematic of the  $\text{UiO-66-(COOH)}_2$  used for stabilizing Zn anode. (b) Ion conductivity of  $\text{UiO-66}$  and  $\text{UiO-66-(COOH)}_2$ . (c) Plating/stripping overpotential of symmetric cells for bare Zn,  $\text{UiO-66@Zn}$ ,  $\text{UiO-66-(COOH)}_2@Zn$ . Reproduced from ref. 67 with permission from Elsevier Inc., copyright 2023. (d) Schematic diagram of coating on a Zn anode. (e) Cycling stability of plating/stripping in a symmetric cell with  $\text{Zr-MOF80 + PVDF-HFP}$  or  $\text{Zr-MOF80 + PVDF}$ . Reproduced from ref. 68 with permission from Elsevier Inc., copyright 2022.

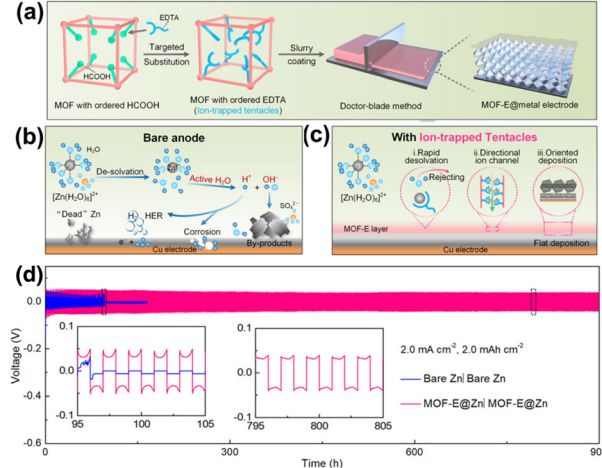


**Fig. 7** (a) Schematic of ordered HCOOH in MOF-808 be substituted by EDTA to form MOF-808 with ordered EDTA (MOF-E) and the process of electrode preparation. Schematic of Zn deposition on (b) bare Cu and (c) MOF-E@Cu. (d) Zn plating/stripping in a symmetric cell with MOF-E@Zn and bare Zn. Reproduced from ref. 69 with permission from John Wiley & Sons, copyright 2023.

molecules from the MOF channels, enabling the construction of a super-saturated electrolyte (Fig. 9b). The coordinated ions passing through the MOF channels exhibited different solvation structures compared to those in the bulk electrolyte. Benefiting from the ZIF-7 layer on Zn anode, the assembled

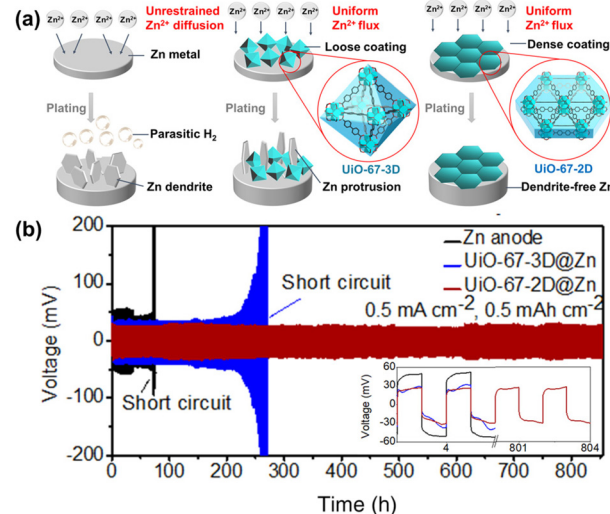


**Fig. 8** (a) Scheme of anode variation and (b) cycling stability of plating/stripping in a symmetric cell with  $\text{UiO-67-2D@Zn}$ ,  $\text{UiO-67-3D@Zn}$ , bare Zn. Reproduced from ref. 41 with permission from Springer Nature, copyright 2022.

symmetric cell demonstrated continuous operation for 3000 h at  $0.5 \text{ mA cm}^{-2}$  (Fig. 9c).

ZIF-8, a type of Zn-MOF, has been extensively investigated as a protective layer on Zn anodes to enhance their stability. Various preparation strategies have been employed to regulate

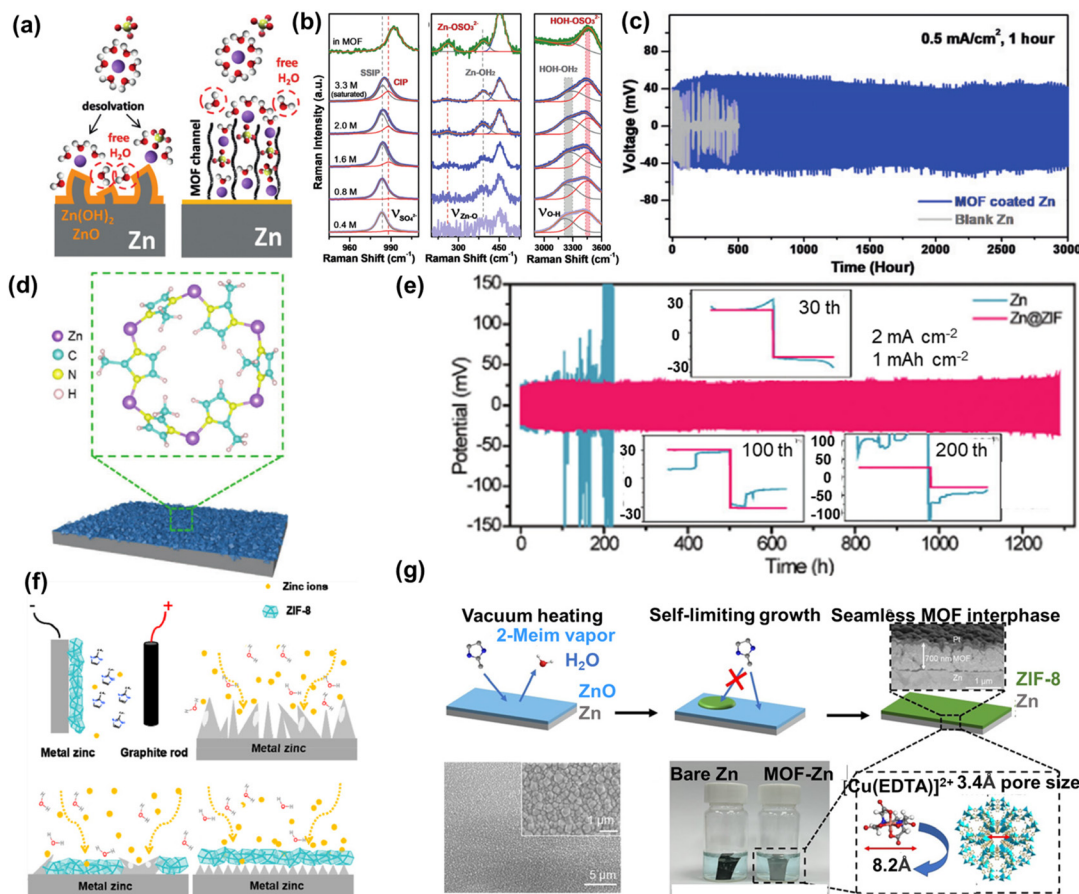


**Fig. 9** (a) Schematic illustration of the surface evolution of Zn. (b) Raman spectroscopy of concentration gradient ZnSO<sub>4</sub> and in MOF channels. (c) Voltage profiles of symmetric cells based on bare Zn foil and MOF coated Zn anodes. Reproduced from ref. 70 with permission from John Wiley & Sons, copyright 2020. (d) Schematic for the Zn@ZIF sample. (e) Voltage profiles of symmetric cells on bare Zn foil and Zn@ZIF anodes. Reproduced from ref. 73 with permission from American Association for the Advancement of Science, copyright 2020. (f) Schematic of electrodeposition ZIF-8 on Zn. Reproduced from ref. 75 with permission from American Chemical Society, copyright 2021. (g) Schematic of the reaction process for the MOF interphase. Reproduced from ref. 76 with permission from Elsevier Inc., copyright 2023.

the morphology of ZIF-8 to optimize its protective properties. Pu *et al.*<sup>71</sup> introduced ZIF-8@Zn by coating MOF(ZIF-8) ink on the Zn surface as a protective layer. Distinctive porous ZIF-8 facilitated homogeneous Zn stable stripping/plating. In addition to directly coating ZIF-8 ink onto the Zn surface, *in situ* growth of a ZIF-8 layer on the Zn substrate provided a porous structure that enabled the uniform deposition of Zn<sup>2+</sup> ions and close contact with the Zn anodes. This promoted dendrite-free operation of the Zn anode. For example, Liu *et al.*<sup>72</sup> designed a ZIB electrode/electrolyte system using Zn-MOF (ZIF-8)/Zn as a microporous substrate and (CF<sub>3</sub>SO<sub>3</sub>)<sub>2</sub>Zn as the electrolyte. This design enabled even charge/discharge processes and facilitated ion diffusion throughout the system. Liu *et al.*<sup>73</sup> performed *in situ* growth of a 1 μm thick ZIF-8 layer as an ion modulation layer, which regulated the diffusion of Zn<sup>2+</sup> ions on the anodes (Fig. 9d). Well-ordered nanochannels and the presence of N species promote the rapid diffusion of Zn<sup>2+</sup> ions, which is beneficial for mitigating the underlying tip effect. ZIF-8 would homogenize the distribution of Zn<sup>2+</sup> flux, thereby facilitating dendrite-free and even deposition of Zn.

The symmetric battery demonstrated stable cycling for 1200 h at 2 mA cm<sup>-2</sup>, 1 mA h cm<sup>-2</sup> (Fig. 9e). To solve the HER and dendrite growth of Zn anodes, He *et al.*<sup>74</sup> prepared a MOF (ZIF-L) layer with 3 μm on the Zn surface (Zn@ZIF-L) through an *in situ* synthesis method. Zn@ZIF-L was obtained by immersing a polished Zn plate in 2-methylimidazole solution and adding HNO<sub>3</sub> for a 6 h reaction. Compared to the above-mentioned ZIF-8 (ZIF-8@Zn), it was found that the thickness of the ZIF-8 layer on Zn anode increases with the addition of HNO<sub>3</sub>.

In addition to the previously reported methods of directly coating ZIF-8 slurry or *in situ* growth of ZIF-8 onto the Zn anode, other synthetic methods have also been employed. For instance, Zeng *et al.*<sup>75</sup> utilized a novel electrodeposition technique to construct a tightly adhering ZIF-8 layer on the Zn anode (Fig. 9f). Besides the electrodeposition method, the vapor-solid reaction between 2-methylimidazole vapor and the ZnO layers was presented by Luo *et al.*<sup>76</sup> (Fig. 9g). A non-defect-laden and molecule-sieving ZIF-8 interface, with a thickness of 0.7 μm, was formed on the surface of Zn. This MOF

layer effectively prevented direct contact between the Zn anode and the aqueous electrolyte, which facilitated the desolvation of  $Zn^{2+}$  ions.  $Zn^{2+}$  ion deposition on the MOF-coated anode exhibited a preferred orientation along the (002) plane.

A variety of Zn-based MOFs have been proposed as protective coatings for the Zn anode to prevent dendrite formation and the HER, taking advantage of the promising developments in ZIBs achieved by ZIFs.<sup>77–80</sup> These MOFs have demonstrated superior lifespan compared to bare anodes when used in symmetric ZIBs. However, these Zn-based MOFs are synthesized through the assembly of soft divalent  $Zn^{2+}$  ions with imidazole or carboxylate ligands, resulting in an unstable MOF in aqueous solutions. Thus, the framework of these MOFs is prone to collapse in aqueous solutions during battery testing, resulting in the formation of zinc oxide or zinc hydroxide which acts as a protective layer for the Zn anode. Several studies have highlighted the effectiveness of zinc oxide and zinc hydroxide as protective coatings for Zn electrodes.<sup>81–83</sup>

Water-sensitive MOFs can be applied in ZIBs using the two-electrolyte strategy. Cao *et al.*<sup>84</sup> developed a method in which the Zn anode was separated from the  $Zn(TFSI)_2\text{-H}_2\text{O}$  aqueous electrolyte by coating a MOF layer on Zn and then  $Zn(TFSI)_2\text{-tris}(2,2,2\text{-trifluoroethyl})$  phosphate (TFEP) organic electrolyte trapped into the pores of organophilic MOF  $Cu_3(BTC)_2$  (also known as HKUST-1, Fig. 10a–c). Since HKUST-1 was occupied by the organic electrolyte  $Zn(TFSI)_2\text{-TFEP}$ , the immiscibility between the organic electrolyte and the aqueous phase electrolyte prevented water from entering the pores of HKUST-1. The  $Zn(TFSI)_2\text{-TFEP}@HKUST-1$  coated Zn anodes were assembled into a Zn symmetric cell to achieve dendrite-free Zn plating/stripping for 700 h with a CE of 99.9% (Fig. 10d).

Compared to MOFs, COF materials are constructed with robust covalent bonds between organic building blocks. Covalent bonds are known for their excellent chemical and electrochemical stability, particularly in aqueous environments, which contributes to enhanced cycling stability of COF materials. Thus, COFs have found extensive application as a protective layer for Zn anodes. For instance, Park *et al.*<sup>56</sup> developed nanoporous and flexible DIP D COF films with a thickness of 50 nm, which could easily self-assemble on Zn anodes in a simple dip-coating procedure. COF films induce even  $Zn^{2+}$  ion deposition and promote a dendrite-free anode during anode plating/stripping processes, suppressing inactive by-product formation. In contrast to using a dip-coating method to grow flexible DIP D COF on Zn anodes, Zhao *et al.*<sup>38</sup> used a pulling method in acetone, with Zn foil as the substrate to fabricate the FCOF@Zn anode after drying. The ultrathin, fluorinated 2D porous FCOF films functioned as an effective Zn anode protective layer. The fluorine atoms in the FCOF exhibit a strong binding interaction with Zn and interact prominently with the (002) plane, resulting in a more stable bond with the (002) plane. The presence of fluorine atoms regulates the horizontal arrangement of Zn electrodeposits (Fig. 11a). In addition, FCOF nanochannels promote ion transmission and tightly adhere to the Zn surface, preventing electrolyte infiltration and reducing aqueous electrolyte corrosion. The 2D COF film (100 nm thickness) is flexible and can buffer volume changes during charging/discharging (Fig. 11b). The symmetric cell with the FCOF@Zn anode outperformed the DIP D COF@Zn anode, exhibiting a longer lifespan of 750 h at 40 mA cm<sup>-2</sup> (Fig. 11c).

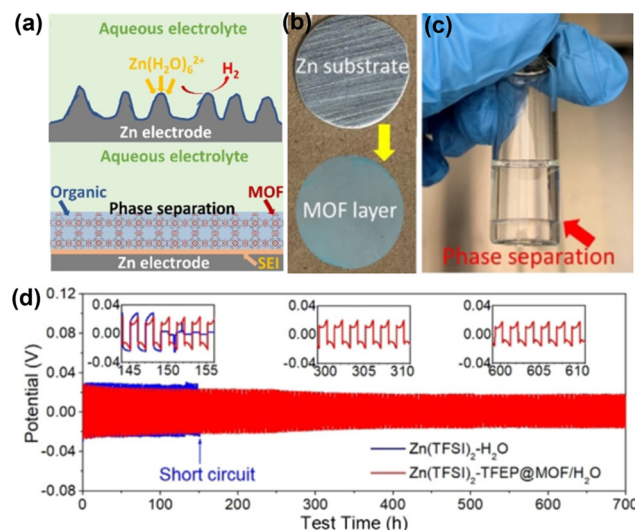


Fig. 10 (a) Scheme of the surface structure and surface reaction of Zn anodes. (b) Photographs of the zinc electrode before and after surface coating of MOF layer. (c) Phase separation of aqueous  $Zn(TFSI)_2\text{-H}_2\text{O}$  electrolyte (on the top) from organic  $Zn(TFSI)_2\text{-TFEP}$  (on the bottom). (d) Galvanostatic Zn plating/stripping in symmetrical cells at  $0.5\text{ mA cm}^{-2}$  and  $0.5\text{ mA h cm}^{-2}$ . Reproduced from ref. 84 with permission from John Wiley & Sons, copyright 2020.

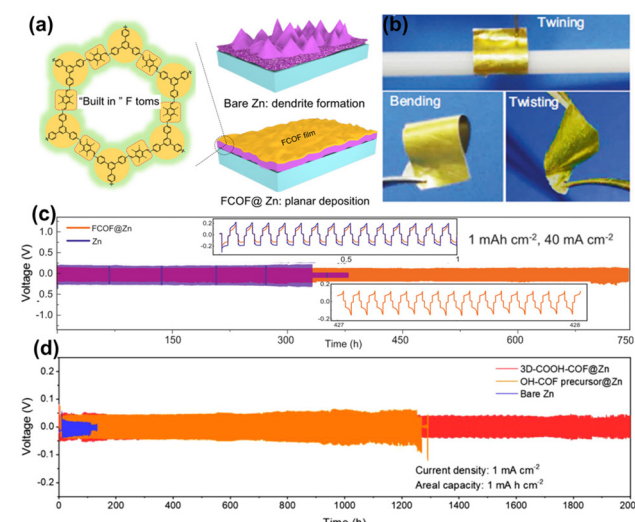


Fig. 11 (a) Mechanism comparison of the Zn deposition processes. (b) Pictures of flexibility FCOF. (c) Stability test for Zn symmetric cells at  $1\text{ mA h cm}^{-2}$ ,  $40\text{ mA cm}^{-2}$ . Reproduced from ref. 38 with permission from Springer Nature, copyright 2021. (d) Long-term cycling performance of Zn plating/stripping in symmetric cells. Reproduced from ref. 39 with permission from Elsevier Inc., copyright 2022.

Functionalizing COFs with other electronegative functional groups can enhance Zn anode stability by promoting strong interactions between the functional groups and Zn atoms, similar to the zincophilic behavior of F atoms. Zhao *et al.*<sup>85</sup> synthesized a zincophilic COF (TpPa-SO<sub>3</sub>H) to stabilize the Zn anode. The incorporation of -SO<sub>3</sub>H groups on the COF film promotes even deposition and fast transport of Zn<sup>2+</sup> ions, resulting in dendrite-free Zn anodes. Furthermore, the TpPa-SO<sub>3</sub>H layer acts as a barrier, preventing the Zn anode from reacting with the electrolyte and inhibiting dendrite growth and the HER. Similar to -SO<sub>3</sub>H, -COOH is also a typical electronegative functional group, and Wu *et al.*<sup>39</sup> engineered thin and homogeneous -COOH functionalized 3D COF protection films as the Zn anode protective layer used in ZIBs. The -COOH functionalized 3D-COF film, with its abundant -COOH groups and uniform nanochannels, enables fast Zn<sup>2+</sup> transmission while hindering SO<sub>4</sub><sup>2-</sup> passage. This promotes high Zn<sup>2+</sup> transfer efficiency and prevents dendrite growth on the Zn anode. The film tightly covers the Zn anodes effectively but blocks electrolyte reactions and reduces corrosion and the HER. The symmetric cell based 3D-COOH-COF@Zn demonstrates stable operation for 2000 h at 1 mA cm<sup>-2</sup> (Fig. 11d).

Besides, Guo *et al.*<sup>55</sup> developed PVC-Zn-AAn-COF@Zn anodes by drop-casting a COF-based PVC slurry onto Zn plates. The unique pore structure of Zn-AAn-COF, which contains zincophilic groups (C=N and C=O), helps prevent the HER and control the movement of Zn<sup>2+</sup> ions in ZIBs by excluding solvated water in the electrolyte (Fig. 12a). And the assembled symmetric cells can work smoothly over 3000 cycles (overpotential < 79.1 mV) at 20 mA cm<sup>-2</sup> (Fig. 12b). In addition, Guo *et al.*<sup>86</sup> utilized a novel electrospray technology to create a protective coating of hetero-metallic cluster COF (MCOF-Ti<sub>6</sub>Cu<sub>3</sub>) nanosheets (MNC) on the Zn anode. The MCOF coating offers advantages such as rapid deposition kinetics and uniform distribution of the electric field, enhancing the performance and durability of the Zn anode (Fig. 12c). The MNC@Zn symmetric cell demonstrated a low overpotential of 72.8 mV during operation. Furthermore, it exhibited excellent long-term stability, operating continuously for 10 000 cycles at 1 mA h cm<sup>-2</sup>, 20 mA cm<sup>-2</sup> (Fig. 12d). Apart from developing various fabrication methods, Hu *et al.*<sup>87</sup> introduced a unique flower-like, high stability, and acid-base resistant 2D COF-H topography as the SEI to inhibit surface corrosion and suppresses dendrite-growth on Zn anode. The uniform distribution of Zn<sup>2+</sup> in channels and the strong affinity of electron-rich sites such as alkynyl, ketone, and enamine groups in COF-H to Zn<sup>2+</sup> were beneficial. Recently, Aupama *et al.*<sup>88</sup> exploited COF-based artificial solid SEI layers (HqTp and BpTp) to protect Zn anodes. Ketone and imine functional groups in COFs can coordinate with Zn<sup>2+</sup>, causing uniform Zn<sup>2+</sup> deposition. The COF layers also decrease Zn<sup>2+</sup> desolvation energy and reduce the Zn nucleation overpotential. Besides, a robust framework of the COF film can suppress side reactions, such as Zn corrosion and the HER, achieving high-performance Zn anode in ZIBs.

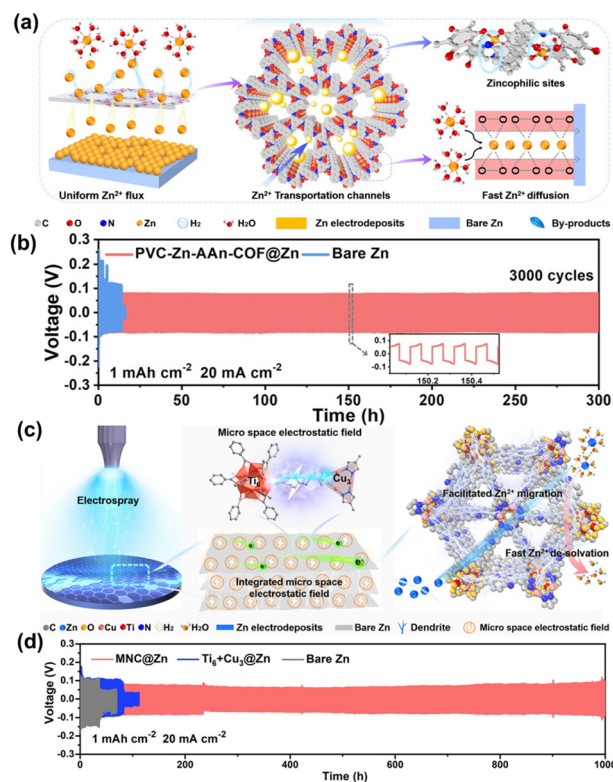
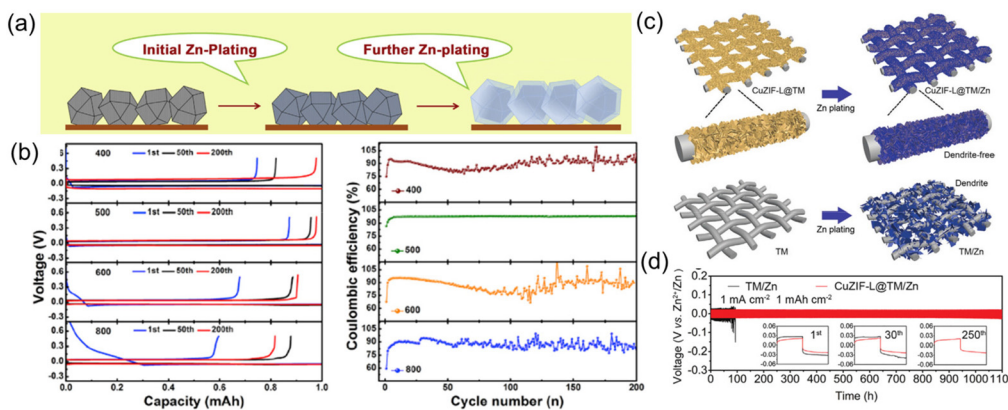


Fig. 12 (a) Mechanism comparison of the Zn deposition on Zn-COF@Zn anode. (b) Cycling stability of symmetrical cells on bared Zn and PVC-Zn-AAn-COF@Zn. Reproduced from ref. 55 with permission from John Wiley & Sons, copyright 2022. (c) Schematic of electrospray preparation process of MNC for ZMBs Zn coating. (d) Cycling stability of a symmetric cell. Reproduced from ref. 86 with permission from John Wiley & Sons, copyright 2023.

### 3.2 MOFs/COFs as porous Zn hosts

It is widely acknowledged that the use of Zn hosts can effectively impede dendrite growth and facilitate homogeneous deposition of Zn<sup>2+</sup> ions, thereby achieving stable cycling performance in ZIBs. Wang *et al.*<sup>89</sup> used annealed ZIF-8 at 500 °C as a host material in a Zn battery (Fig. 13a). The porous structure of the annealed ZIF-8 and the presence of a small amount of Zn (0) effectively suppressed the HER, resulting in a high CE close to 100% and long-term cycle life (Fig. 13b). Annealing ZIF-8 at 500 °C produced a substantial amount of thermally reduced Zn(0) within the framework. The trace quantity of Zn(0) plays a vital role in facilitating uniform nucleation during Zn plating and inhibiting the HER triggered by water decomposition. Similarly, Lei *et al.*<sup>90</sup> used ZIF-8 annealed at 500 °C as host materials to achieve stable and dendrite-free Zn anodes. ZIF-8-derived carbon (ZIF-8-C) served as the cathode material in Zn-ion capacitors. The solid-state Zn@annealed ZIF-8/ZIF-8-C ZICs successfully powered LEDs and smartwatches, showing promise for practical applications. Tao *et al.*<sup>91</sup> designed a unique anode host structure named CuZIF-L@TM for ZIBs. Copper dispersed in the interconnected leaf-like ZIF-L nanoflakes to create a



**Fig. 13** (a) Schematic illustration of Zn plating. (b) Polarization for various temperature treated ZIF-8 electrodes tested at  $2.0 \text{ mA cm}^{-2}$  (up), CE of different electrodes (down). Reproduced from ref. 89 with permission from Elsevier Inc., copyright 2019. (c) Schematic for Zn depositions on CuZIF-L@TM and TM during plating. (d) Cycling performances of symmetric cells based on CuZIF-L@TM/Zn or TM/Zn electrodes. Reproduced from ref. 91 with permission from John Wiley & Sons, copyright 2022.

unique 3D network structure that helped homogenize the distribution of the electric field. The CuZIF-L nanoflakes have a high surface area and sufficient void space, enabling effective electrolyte contact and accommodating electrode volume changes. The presence of zincophilic sites in the CuZIF-L@TM configuration ensures uniform  $\text{Zn}^{2+}$  ion deposition without dendrite formation (Fig. 13c). The symmetric cell assembled using the CuZIF-L@TM/Zn electrode showed stable Zn plating/stripping performance for over 1100 h at  $1 \text{ mA cm}^{-2}$  (Fig. 13d).

### 3.3 MOFs/COFs as separators, solid-state electrolytes, or electrolyte additives

Stable Zr-MOF is not only used as a protective layer on Zn anodes but also applied in the separator for ZIBs. Wang *et al.*<sup>62</sup> designed a Janus separator based on a Zr-MOF(MOF-808) and rGO, where the anionic MOF-808 provides a  $\text{Zn}^{2+}$  rich layer and sub-nano tunnels to ensure even  $\text{Zn}^{2+}$  flux and electron transmission (Fig. 14a). The MOF-808/rGO layers are evenly deposited on a polymer membrane, forming a flat surface with a combined thickness of about 25  $\mu\text{m}$  (Fig. 14c-g). The plating/stripping processes were stable for up to 500 h at 0.5 and  $2 \text{ mA cm}^{-2}$  (Fig. 14b). The use of MOF-808/rGO separator in symmetric cells with Zn anodes prevented dendrite formation and suppressed corrosion. In comparison, the Zn anode with a pristine separator exhibited dendrite growth after 100 cycles at  $2 \text{ mA cm}^{-2}$  (Fig. 14f and g). Song *et al.*<sup>92</sup> reported a functionalized Zr-MOF separator (UiO-66-GF) used in ZIBs. The assembled symmetric cell with UiO-66-GF separator exhibited a long cycle life of up to 1650 h at  $2.0 \text{ mA cm}^{-2}$  with high CE and low polarization of 39 mV (Fig. 14h). Compared to the MOF-808/rGO separator, UiO-66-GF was more effective for the stabilization of ZIBs. Naskar *et al.*<sup>93</sup> utilized a ZIF-8 layer as a separator with a robust nano-porous structure containing Zn-N-based polyhedral clusters. This design effectively restricted  $\text{Zn}^{2+}$  movement at the cathode during discharging, allowing improved diffusion through open channels during charging.

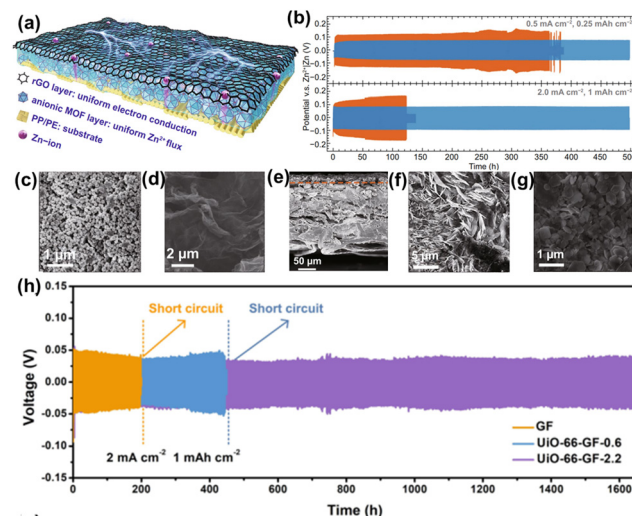


**Fig. 14** (a) Schematic of the Janus separator. (b) Cycling performance of the Zn//Zn symmetric cells with different separators. SEM for the (c) MOF and (d) rGO layer and the (e) cross-sectional image of the Janus separator. SEM of the Zn surface after cycling 100th time with  $2 \text{ mA cm}^{-2}$  using (f) pristine and (g) Janus separator. Reproduced from ref. 62 with permission from Springer Nature, copyright 2021. (h) Zn plating/stripping performances in a symmetric cell with different separators. Reproduced from ref. 92 with permission from Springer Nature, copyright 2022.

As a result, the  $\text{Zn}^{2+}$  ion storage and cycling stability were enhanced.

Wang *et al.*<sup>94</sup> used Zr-MOF (MOF-808) to create a single-ion  $\text{Zn}^{2+}$  solid-state electrolyte (SSE) for stable ZIBs. The modified MOF-808-based SSE exhibited high ionic conductivity,  $\text{Zn}^{2+}$  transference number, and mechanical electrochemical stability, enabling dendrite-free and reversible plating/stripping of Zn (Fig. 15a). The SSE enables uniform and flat deposition of  $\text{Zn}^{2+}$ , which benefits long-term plating/stripping (Fig. 15b). Besides, Park *et al.*<sup>95</sup> utilized stable Zn sulfonated COF

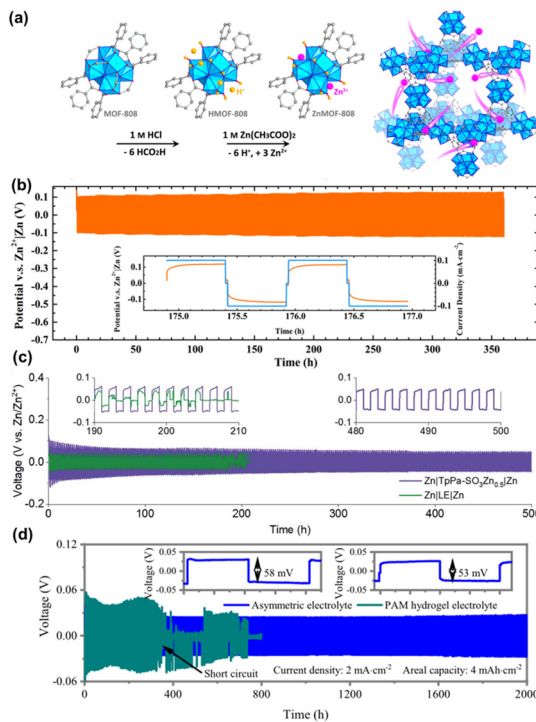


**Fig. 15** (a) Crystal structure and scheme for the synthetic process of ZnMOF-808. (b) Zn plating/stripping performance of a symmetric cell at  $0.1 \text{ mA cm}^{-2}$ . Reproduced from ref. 94 with permission from Elsevier Inc., copyright 2019. (c) Zn plating/stripping performances of  $\text{Zn}|\text{TpPa-SO}_3\text{Zn}_{0.5}|\text{Zn}$  and  $\text{Zn}|2 \text{ M ZnSO}_4|\text{Zn}$  cells. Reproduced from ref. 95 with permission from Royal Society of Chemistry, copyright 2020. (d) Cycling stability of Zn//Zn symmetric cells with different electrolytes. The insets show at the 5th and 1000th cycles. Reproduced from ref. 97 with permission from Springer Nature, copyright 2023.

(TpPa-SO<sub>3</sub>Zn<sub>0.5</sub>) as SSE in ZIBs. Delocalised-SO<sub>3</sub> is covalently linked to directional pores in TpPa-SO<sub>3</sub>Zn<sub>0.5</sub> by its  $\beta$ -ketamine linkages to achieve single Zn<sup>2+</sup> ion transport. The TpPa-SO<sub>3</sub>Zn<sub>0.5</sub> promotes redox reliability and stability for Zn plating/stripping. This enables the symmetric cell to be stable to operate for 500 h at  $0.1 \text{ mA cm}^{-2}$ ,  $0.1 \text{ mA h cm}^{-2}$  (Fig. 15c). Gong *et al.*<sup>96</sup> suggested the use of ZIF-8 as an electrolyte additive for ZIBs to inhibit dendrite growth during Zn reversible plating/stripping in ZIBs. The binding energy for Zn<sup>2+</sup> was calculated through DFT and it was concluded that the movement of Zn<sup>2+</sup> depends on the adsorption capacity of ZIF-8. The highest stability can be attained by incorporating ZIF-8 additives at a concentration of  $4 \text{ mg mL}^{-1}$  in 2 M ZnSO<sub>4</sub> electrolyte solution. Chen *et al.*<sup>97</sup> designed asymmetric electrolyte with a thickness of  $210 \mu\text{m}$  using porphyrin paddlewheel-like 2D MOF combined with polyacrylamide gel electrolyte to realize a highly reversible dendrite-free and corrosion-resistant Zn anode. The cycling stability of the Zn anode was tested by symmetric cells using different gel electrolytes. The side of the MOF layer toward the Zn anode can avoid H<sub>2</sub>O reaction with the Zn anode. Therefore, the HER and dendrite growth were depressed effectively, resulting in outstanding cycling stability over 2000 h (Fig. 15d).

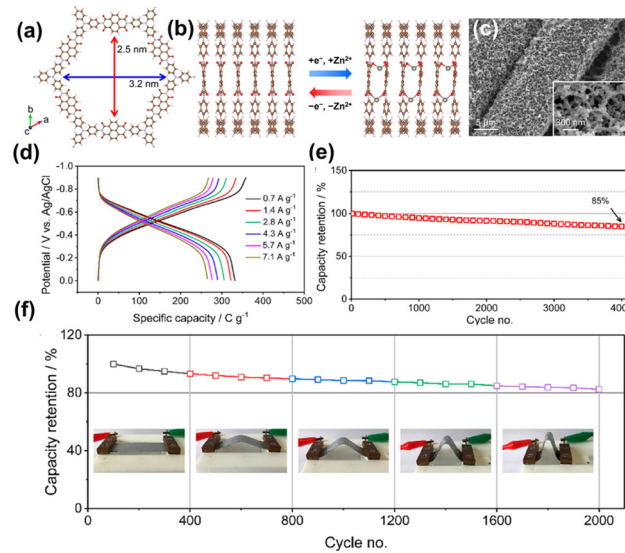


**Fig. 16** (a) 2D PI-COF structure. (b) Zn<sup>2+</sup>-storage process in PI COF. (c) SEM images for PI-COF. (d) Charge/discharge curves. (e) Cycling performance of the PI-COF electrode at  $10 \text{ mV s}^{-1}$ . (f) Cycling performance of PI-COF//MnO<sub>2</sub> battery at  $0.1 \text{ V s}^{-1}$  in different deformation states. Reproduced from ref. 48 with permission from American Chemical Society, copyright 2020.

### 3.4 MOFs/COFs as Zn metal-free anodes

Distinct from the previously discussed Zn-based anodes, Yu *et al.*<sup>48</sup> presented a Zn metal-free anode for ZIBs based on a 2D polyarylimide COF (PI-COF). The PI-COF served as a direct anode in ZIBs and demonstrates a high-capacity Zn<sup>2+</sup> storage capability with a two-step Zn<sup>2+</sup> storage mechanism (Fig. 16a and b). The SEM images showed entangled networks of PI-COF/CNTs bundles (Fig. 16c). The ordered pore channels of PI-COF allowed high accessibility of the redox-active  $-\text{C}=\text{O}$  and low energy barrier ion spread. The PI-COF electrode displayed a capacity of  $92 \text{ mA h g}^{-1}$  at  $0.7 \text{ A g}^{-1}$  (Fig. 16d). The PI-COF electrode shows a capacity retention of 85% after 4000 charge/discharge cycles tested at  $10 \text{ mV s}^{-1}$  with CV testing (Fig. 16e). In addition, the cycling stability of PI-COF//MnO<sub>2</sub> full battery test under different deformation states displays a capacity retention of 82.5% after 2000 cycles, proving that the assembled PI-COF//MnO<sub>2</sub> has great promise in the application for flexible and wearable electronics (Fig. 16f).

## 4. Structure–property relationship

We have summarized the structures and properties of previously discussed MOFs/COFs in Table S1.<sup>†</sup> To reveal the effect of MOF/COF structures on their electrochemical performances, the relationship between the key structural parameters of MOFs/COFs and the performance of ZIBs is displayed in Fig. S1.<sup>†</sup> In this section, we will analyze the effect of pore size, BET surface area, surface functional groups and morphology of MOFs/COFs on their performance as Zn anodes in ZIBs.

#### 4.1 Effect of MOF/COF pore size and BET surface area

In theory, the properties of MOFs and COFs (*e.g.*, pore size and BET surface area) affect the  $Zn^{2+}$  diffusion along the porous channels, therefore controlling the electrochemical properties of Zn anodes. We carefully analyzed the effect of pore size and BET surface area on the electrochemical properties of Zn anodes including Zn deposition/stripping overpotential,  $Zn^{2+}$  transference number, and  $Zn^{2+}$  conductivity. A linear correlation was observed between the pore sizes of MOFs and the  $Zn^{2+}$  transference number (Fig. S1†). This trend seems counter-intuitive as the small pore size of MOFs/COFs may restrict the diffusion of counter-anions and increase the  $Zn^{2+}$  transference number. We speculate that the  $Zn^{2+}$  transference number measured for MOF/COF-coated Zn anodes is an average of solid-phase ( $Zn^{2+}$  diffuse through MOFs/COFs) and solution-phase diffusion ( $Zn^{2+}$  diffuse through aqueous electrolytes between MOF/COF particles). Therefore, increasing the pore sizes of MOFs/COFs may facilitate the  $Zn^{2+}$  diffusion through the porous channels of MOFs/COFs, thus increasing the  $Zn^{2+}$  transference number. In addition, the MOFs generally possess lower overpotential than COFs, highlighting the critical role of metals in inducing Zn nucleation and deposition (Fig. S1†). On the other hand, the impact of porosity parameters (BET surface area/pore size) on the overpotential and  $Zn^{2+}$  conductivity appears to be inconspicuous. For instance, variations in overpotential from 30 mV to 55 mV under 1 mA h cm<sup>-2</sup> are observed in the case of the same MOF material (ZIF-8) assembled using different methods (drop-casting, *in situ* growth). These findings suggest that the local pore structure of MOFs/COFs has a relatively lower impact on the performance of ZIBs compared to the surface properties and morphology of MOF/COF nanoparticles.

#### 4.2 Effect of surface functional groups on MOFs/COFs

Polar and zincophilic functional groups (atoms) were shown to improve the electrochemical performances of MOF/COF-based Zn anodes. For example, -COOH functionalized COF (3D-COOH-COF) exhibited lower overpotential, higher  $Zn^{2+}$  transfer number, higher  $Zn^{2+}$  conductivity, and better cycling stability (50 mV, 2000 h, 1 mA cm<sup>-2</sup>, 1 mA h cm<sup>-1</sup>,  $\tau_{Zn} = 0.82$ ; 0.26 mS cm<sup>-1</sup>) than the -OH functionalized COF (OH-COF, 60 mV, 1272 h, 1 mA cm<sup>-2</sup>, 1 mA h cm<sup>-2</sup>,  $\tau_{Zn} = 0.69$ ; 0.20 mS cm<sup>-1</sup>).<sup>39</sup> Similarly, UiO-66-(COOH)<sub>2</sub>, a hydrophilic MOF with -COOH as a zincophilic and anion-blocking functional group, shows an improved  $Zn^{2+}$  transfer number and cycling stability than unmodified UiO-66.<sup>67</sup> In addition to -COOH, -SO<sub>3</sub>H group functionalized TpPa-SO<sub>3</sub>H also demonstrated increased electrochemical performances in ZIBs.

#### 4.3 Effect of MOF/COF morphology

The morphology of MOFs/COFs plays a crucial role in regulating the contact between MOFs/COFs and Zn surface. Generally, 2D MOF/COF nanosheets/nanoplates can tightly coat on the Zn anode, preventing undesirable cracks from occurring due to the volume change of the Zn anode during

long-term plating/stripping processes. This seamless layer of MOFs/COFs acts as a physical barrier, preventing the electrolyte from infiltrating into the Zn anode, inhibiting the reaction of the electrolyte with Zn and reducing the HER and corrosion. Furthermore, the robust protective layer inhibits dendritic growth with mechanical force, improving the stability of the Zn anode. For example, UiO-67-2D nanosheets show higher protective performance than UiO-67-3D nanoparticles when applied as Zn anode coating materials.<sup>41</sup> Similarly, 2D-COFs can form films that tightly adhere to the Zn anode which act as a stable artificial interface layer to prevent the HER and corrosion caused by electrolyte reaction with the Zn anode. Zn anode plating/stripping reversibility and the  $Zn^{2+}$  ion diffusion behavior can be effectively regulated by the COF layer.<sup>38</sup>

## 5. Conclusions and perspectives

MOF/COF-based materials possess great potential for  $Zn^{2+}$  ion energy storage applications. We have categorized and discussed possible solutions based on MOF/COF materials to address the problems of Zn anodes. By analyzing the literature, we propose the following suggestions and strategies to further optimize MOF/COF-based Zn anodes.

#### 5.1 Engineering the surface properties of MOFs/COFs

Previous works have highlighted the importance of surface polarity and zincophilic sites on the Zn anode performances. Currently, a series of functional groups including -F, -CF<sub>3</sub>, -NH<sub>2</sub>, -COOH, -OH, and -SO<sub>3</sub>H have been incorporated into MOFs/COFs for improved  $Zn^{2+}$  conductivity and long-term plating/stripping stability. With the development of MOF/COF synthesis and modification methods, we expect that more functional groups can be introduced. For example, weak coordinating counter-anions such as sulfonimide-functional groups can be potentially incorporated into MOFs/COFs to improve the ionic conductivity and realize single-ion electrolytes. In addition, multivariable MOFs/COFs have emerged as versatile platforms for the design of advanced materials. Multivariable MOFs/COFs possess a higher degree of complexity compared to conventional MOFs/COFs as they incorporate multiple variables or components into their structures. By incorporating multiple functional groups with synergistic effects for  $Zn^{2+}$  transport, nucleation, and deposition, we expect that the resulting MOFs/COFs will exhibit enhanced properties in ZIBs than the current single-component MOFs/COFs.

#### 5.2 Regulating the morphology of MOFs/COFs

The control of MOF/COF morphology is crucial for the formation of crack-free films in Zn anode coatings. The recent advancements in 2D MOF nanosheets and MOF glasses offer new opportunities for fabricating MOF/COF-coated Zn anodes. Exfoliated 2D MOF nanosheets can be selectively oriented and deposited onto the substrate, while certain MOFs can be transformed into MOF glasses, enhancing processability while maintaining porosity. These approaches have been success-

fully utilized for fabricating crack-free membranes in gas separation applications and can potentially be adapted for the fabrication of MOF/COF-coated Zn anodes, improving the contact between the framework materials and Zn surface. Moreover, the combination of MOFs/COFs with other 2D layered materials, such as Mxene and graphene oxide (GO), enables the creation of composite materials with tunable morphologies and enhanced performances in ZIBs.

### 5.3. Improving the stability of MOFs

The stability of MOFs in ZIBs is a major concern in the study of MOF-based Zn anodes. Although many MOFs have been explored and some of them show promising performances in ZIBs, their framework stability after cycling is often overlooked. If MOFs are decomposed into metal oxides/hydroxides during battery tests, the MOF-based surface engineering and mechanistic discussions are rendered invalid. To ensure stability, high valent and redox inert metals ( $Zr^{4+}$ ,  $Ti^{4+}$ , and  $Al^{3+}$ ) are recommended. We also recommend that future researchers examine the structure of MOFs after battery tests by PXRD.

The crystalline MOFs/COFs with well-defined structures provide an ideal platform for mechanistic studies by *in situ* techniques and theoretical calculations. By analyzing the relationship between MOF/COF structures and their properties in ZIBs, we expect to extract key descriptors for electrochemical performance. These insights will facilitate the identification of key descriptors for optimizing electrochemical performance, guiding the rational design and screening of MOFs/COFs for future ZIB applications. Challenges exist in using MOFs/COFs for ZIBs. MOFs/COFs often possess a fragile and crystalline structure, making them susceptible to degradation when the repeated expansion and contraction of the electrode material during charge/discharge. Some MOFs/COFs have complex synthesis processes and expensive ligands, which can increase the costs of ZIBs. Currently, only a limited number of MOFs/COFs have been explored. Despite being in the early stages, researchers are actively working to overcome these limitations. The structural diversity and functional tunability of MOFs/COFs indicate a promising future for their application in Zn metal anodes, ultimately leading to the development of stable ZIBs suitable for practical use.

## Conflicts of interest

There are no conflicts to declare.

## Acknowledgements

This work was supported by the Natural Science Foundation of China (No. 22271141, 52178219) and the Natural Science Foundation of Jiangsu Province (BK20220765).

## References

- 1 D. Yang, Y. P. Zhou, H. B. Geng, C. T. Liu, B. Lu, X. H. Rui and Q. Y. Yan, Pathways towards high energy aqueous

rechargeable batteries, *Coord. Chem. Rev.*, 2020, **424**, 213521.

- 2 D. Xu, M. Liang, S. Qi, W. Sun, L. P. Lv, F. H. Du, B. Wang, S. Chen, Y. Wang and Y. Yu, The Progress and Prospect of Tunable Organic Molecules for Organic Lithium-Ion Batteries, *ACS Nano*, 2021, **15**, 47–80.
- 3 V. Blay, R. E. Galian, L. M. Muresan, D. Pankratov, P. Pinyou and G. Zampardi, Research Frontiers in Energy-Related Materials and Applications for 2020–2030, *Adv. Sustainable Syst.*, 2020, **4**, 1900145.
- 4 T. Wei, J. H. Lu, M. T. Wang, C. Sun, Q. Zhang, S. J. Wang, Y. Y. Zhou, D. F. Chen and Y. Q. Lan, MOF-Derived Materials Enabled Lithiophilic 3D Hosts for Lithium Metal Anode - A Review, *Chin. J. Chem.*, 2023, **41**, 1861–1874.
- 5 T. Q. Chen, X. J. Liu, L. Y. Niu, Y. Y. Gong, C. Li, S. Q. Xu and L. K. Pan, Recent progress on metal-organic framework-derived materials for sodium-ion battery anodes, *Inorg. Chem. Front.*, 2020, **7**, 567–582.
- 6 F. Ming, Y. Zhu, G. Huang, A. H. Emwas, H. Liang, Y. Cui and H. N. Alshareef, Co-solvent electrolyte engineering for stable anode-free zinc metal batteries, *J. Am. Chem. Soc.*, 2022, **144**, 7160–7170.
- 7 Y. R. Wang, J. Yin and J. Zhu, Two-Dimensional Cathode Materials for Aqueous Rechargeable Zinc-Ion Batteries (dagger), *Chin. J. Chem.*, 2022, **40**, 973–988.
- 8 L. Zhang, H. W. Liu, W. Shi and P. Cheng, Synthesis strategies and potential applications of metal-organic frameworks for electrode materials for rechargeable lithium ion batteries, *Coord. Chem. Rev.*, 2019, **388**, 293–309.
- 9 Q. Wang, J. Sun and D. Wei, Two-dimensional metal-organic frameworks and covalent organic frameworks, *Chin. J. Chem.*, 2022, **40**, 1359–1385.
- 10 C. Wei, L. Tan, Y. Zhang, S. Xiong and J. Feng, Metal-organic frameworks and their derivatives in stable Zn metal anodes for aqueous Zn-ion batteries, *ChemPhysMater*, 2022, **1**, 252–263.
- 11 H. Hong, X. Guo, J. X. Zhu, Z. X. Wu, Q. Li and C. Y. Zhi, Metal/covalent organic frameworks for aqueous rechargeable zinc-ion batteries, *Sci. China: Chem.*, 2023, **66**, 1–13.
- 12 M. Gopalakrishnan, S. Ganesan, M. T. Nguyen, T. Yonezawa, S. Praserthdam, R. Pornprasertsuk and S. Kheawhom, Critical roles of metal-organic frameworks in improving the Zn anode in aqueous zinc-ion batteries, *Chem. Eng. J.*, 2023, **457**, 141334.
- 13 C. Xu, B. Li, H. Du and F. Kang, Energetic zinc ion chemistry: the rechargeable zinc ion battery, *Angew. Chem., Int. Ed.*, 2012, **51**, 933–935.
- 14 Y. Li, X. Li, H. Duan, S. Xie, R. Dai, J. Rong, F. Kang and L. Dong, Aerogel-structured  $MnO_2$  cathode assembled by defect-rich ultrathin nanosheets for zinc-ion batteries, *Chem. Eng. J.*, 2022, **441**, 136008.
- 15 C. P. Li, X. S. Xie, S. Q. Liang and J. Zhou, Issues and Future Perspective on Zinc Metal Anode for Rechargeable Aqueous Zinc-ion Batteries, *Energy Environ. Mater.*, 2020, **3**, 146–159.
- 16 C. L. Xie, Y. H. Li, Q. Wang, D. Sun, Y. G. Tang and H. Y. Wang, Issues and solutions toward zinc anode in

aqueous zinc-ion batteries: A mini review, *Carbon Energy*, 2020, **2**, 540–560.

17 Z. Yi, G. Chen, F. Hou, L. Wang and J. Liang, Strategies for the stabilization of Zn metal anodes for Zn-ion batteries, *Adv. Energy Mater.*, 2021, **11**, 2003065.

18 S. Cai, G. Chang, J. G. Hu, J. E. Wu, Y. Q. Luo, G. Q. Zou, H. S. Hou and X. B. Ji, N, S-Doped Carbon Dots as Additive for Suppression of Zinc Dendrites in Alkaline Electrolyte, *Chin. J. Chem.*, 2023, **41**, 1697–1704.

19 W. Lu, C. Xie, H. Zhang and X. Li, Inhibition of Zinc Dendrite Growth in Zinc-Based Batteries, *ChemSusChem*, 2018, **11**, 3996–4006.

20 Q. Zhang, J. Luan, L. Fu, S. Wu, Y. Tang, X. Ji and H. Wang, The Three-Dimensional Dendrite-Free Zinc Anode on a Copper Mesh with a Zinc-Oriented Polyacrylamide Electrolyte Additive, *Angew. Chem., Int. Ed.*, 2019, **58**, 15841–15847.

21 J. N. Hao, B. Li, X. L. Li, X. H. Zeng, S. L. Zhang, F. H. Yang, S. L. Liu, D. Li, C. Wu and Z. P. Guo, An In-Depth Study of Zn Metal Surface Chemistry for Advanced Aqueous Zn-Ion Batteries, *Adv. Mater.*, 2020, **32**, 2003021.

22 G. Z. Fang, J. Zhou, A. Q. Pan and S. Q. Liang, Recent Advances in Aqueous Zinc-Ion Batteries, *ACS Energy Lett.*, 2018, **3**, 2480–2501.

23 Z. Cai, Y. Ou, B. Zhang, J. Wang, L. Fu, M. Wan, G. Li, W. Wang, L. Wang, J. Jiang, Z. W. Seh, E. Hu, X. Q. Yang, Y. Cui and Y. Sun, A Replacement Reaction Enabled Interdigitated Metal/Solid Electrolyte Architecture for Battery Cycling at  $20 \text{ mA cm}^{-2}$  and  $20 \text{ mAh cm}^{-2}$ , *J. Am. Chem. Soc.*, 2021, **143**, 3143–3152.

24 D. L. Chao, W. H. Zhou, C. Ye, Q. H. Zhang, Y. G. Chen, L. Gu, K. Davey and S. Z. Qiao, An Electrolytic Zn-MnO<sub>2</sub> Battery for High-Voltage and Scalable Energy Storage, *Angew. Chem., Int. Ed.*, 2019, **58**, 7823–7828.

25 X. Jia, C. Liu, Z. G. Neale, J. Yang and G. Cao, Active Materials for Aqueous Zinc Ion Batteries: Synthesis, Crystal Structure, Morphology, and Electrochemistry, *Chem. Rev.*, 2020, **120**, 7795–7866.

26 W. B. Liu, L. B. Dong, B. Z. Jiang, Y. F. Huang, X. L. Wang, C. J. Xu, Z. Kang, J. Mou and F. Y. Kang, Layered vanadium oxides with proton and zinc ion insertion for zinc ion batteries, *Electrochim. Acta*, 2019, **320**, 134565.

27 X. Li, J. M. Zeng, H. Yao, D. Yuan and L. P. Zhang, Current Advances on Zn Anodes for Aqueous Zinc-Ion Batteries, *ChemNanoMat*, 2021, **7**, 1162–1176.

28 J. H. Cavka, S. Jakobsen, U. Olsbye, N. Guillou, C. Lamberti, S. Bordiga and K. P. Lillerud, A new zirconium inorganic building brick forming metal organic frameworks with exceptional stability, *J. Am. Chem. Soc.*, 2008, **130**, 13850–13851.

29 K. S. Park, Z. Ni, A. P. Cote, J. Y. Choi, R. Huang, F. J. Uribe-Romo, H. K. Chae, M. O'Keeffe and O. M. Yaghi, Exceptional chemical and thermal stability of zeolitic imidazolate frameworks, *Proc. Natl. Acad. Sci. U. S. A.*, 2006, **103**, 10186–10191.

30 S. S. Chui, S. M. Lo, J. P. Charmant, A. G. Orpen and I. D. Williams, A chemically functionalizable nanoporous material [Cu<sub>3</sub>(TMA)<sub>2</sub>(H<sub>2</sub>O)<sub>3</sub>], *Science*, 1999, **283**, 1148–1150.

31 J. Li, X. Jing, Q. Li, S. Li, X. Gao, X. Feng and B. Wang, Bulk COFs and COF nanosheets for electrochemical energy storage and conversion, *Chem. Soc. Rev.*, 2020, **49**, 3565–3604.

32 Y. Li, M. Karimi, Y.-N. Gong, N. Dai, V. Safarifard and H.-L. Jiang, Integration of metal-organic frameworks and covalent organic frameworks: Design, synthesis, and applications, *Matter*, 2021, **4**, 2230–2265.

33 C. S. Diercks and O. M. Yaghi, The atom, the molecule, and the covalent organic framework, *Science*, 2017, **355**, eaal1585.

34 A. P. Côté, A. I. Benin, N. W. Ockwig, M. O'Keeffe, A. J. Matzger and O. M. Yaghi, Porous, crystalline, covalent organic frameworks, *Science*, 2005, **310**, 1166–1170.

35 B. Díaz de Greñu, J. Torres, J. García-González, S. Muñoz-Pina, R. de los Reyes, A. M. Costero, P. Amorós and J. V. Ros-Lis, Microwave-assisted synthesis of covalent organic frameworks: a review, *ChemSusChem*, 2021, **14**, 208–233.

36 Y. Li, B. Zou, A. S. Xiao and H. X. Zhang, Advances of Metal-Organic Frameworks in Energy and Environmental Applications, *Chin. J. Chem.*, 2017, **35**, 1501–1511.

37 P. Xue, C. Guo, L. Li, H. Li, D. Luo, L. Tan and Z. Chen, A MOF-derivative decorated hierarchical porous host Enabling ultrahigh rates and superior long-term cycling of dendrite-free Zn metal anodes, *Adv. Mater.*, 2022, **34**, e2110047.

38 Z. Zhao, R. Wang, C. Peng, W. Chen, T. Wu, B. Hu, W. Weng, Y. Yao, J. Zeng, Z. Chen, P. Liu, Y. Liu, G. Li, J. Guo, H. Lu and Z. Guo, Horizontally arranged zinc platelet electrodeposits modulated by fluorinated covalent organic framework film for high-rate and durable aqueous zinc ion batteries, *Nat. Commun.*, 2021, **12**, 6606.

39 K. Wu, X. S. Shi, F. F. Yu, H. X. Liu, Y. J. Zhang, M. H. Wu, H. K. Liu, S. X. Dou, Y. Wang and C. Wu, Molecularly engineered three-dimensional covalent organic framework protection films for highly stable zinc anodes in aqueous electrolyte, *Energy Storage Mater.*, 2022, **51**, 391–399.

40 Q. Huang, Y. Yang and J. J. Qian, Structure-directed growth and morphology of multifunctional metal-organic frameworks, *Coord. Chem. Rev.*, 2023, **484**, 215101.

41 L. L. Lei, F. F. Chen, Y. L. Wu, J. Shen, X. J. Wu, S. S. Wu and S. Yuan, Surface Coatings of Two-Dimensional Metal-Organic Framework Nanosheets Enable Stable Zinc Anodes, *Sci. China: Chem.*, 2022, **65**, 2205–2213.

42 Y. Zhang, C. Wei, M.-X. Wu, Y. Wang, H. Jiang, G. Zhou, X. Tang and X. Liu, A high-performance COF-based aqueous zinc-bromine battery, *Chem. Eng. J.*, 2023, **451**, 138915.

43 S. Yuan, L. Feng, K. Wang, J. Pang, M. Bosch, C. Lollar, Y. Sun, J. Qin, X. Yang, P. Zhang, Q. Wang, L. Zou, Y. Zhang, L. Zhang, Y. Fang, J. Li and H. C. Zhou, Stable

Metal-Organic Frameworks: Design, Synthesis, and Applications, *Adv. Mater.*, 2018, **30**, e1704303.

44 X. L. Li, S. L. Cai, B. Sun, C. Q. Yang, J. Zhang and Y. Liu, Chemically Robust Covalent Organic Frameworks: Progress and Perspective, *Matter*, 2020, **3**, 1507–1540.

45 S. H. Pang, C. Han, D. S. Sholl, C. W. Jones and R. P. Lively, Facet-Specific Stability of ZIF-8 in the Presence of Acid Gases Dissolved in Aqueous Solutions, *Chem. Mater.*, 2016, **28**, 6960–6967.

46 H. Zhang, M. Zhao and Y. S. Lin, Stability of ZIF-8 in water under ambient conditions, *Microporous Mesoporous Mater.*, 2018, **279**, 201–210.

47 E. M. Johnson, S. Ilic and A. J. Morris, Design Strategies for Enhanced Conductivity in Metal-Organic Frameworks, *ACS Cent. Sci.*, 2021, **7**, 445–453.

48 M. Yu, N. Chandrasekhar, R. K. M. Raghupathy, K. H. Ly, H. Zhang, E. Dmitrieva, C. Liang, X. Lu, T. D. Kuhne, H. Mirhosseini, I. M. Weidinger and X. Feng, A High-Rate Two-Dimensional Polyarylimide Covalent Organic Framework Anode for Aqueous Zn-Ion Energy Storage Devices, *J. Am. Chem. Soc.*, 2020, **142**, 19570–19578.

49 X. Zhang, J. P. Hu, N. Fu, W. B. Zhou, B. Liu, Q. Deng and X. W. Wu, Comprehensive review on zinc-ion battery anode: Challenges and strategies, *InfoMat*, 2022, **4**, e12306.

50 L. Ma, M. A. Schroeder, T. P. Pollard, O. Borodin, M. C. S. Ding, R. M. Sun, L. S. Cao, J. Ho, D. R. Baker, C. S. Wang and K. Xu, Critical Factors Dictating Reversibility of the Zinc Metal Anode, *Energy Environ. Mater.*, 2020, **3**, 516–521.

51 L. S. Wu and Y. F. Dong, Recent progress of carbon nanomaterials for high-performance cathodes and anodes in aqueous zinc ion batteries, *Energy Storage Mater.*, 2021, **41**, 715–737.

52 F. Wang, O. Borodin, T. Gao, X. Fan, W. Sun, F. Han, A. Faraone, J. A. Dura, K. Xu and C. Wang, Highly reversible zinc metal anode for aqueous batteries, *Nat. Mater.*, 2018, **17**, 543–549.

53 D. H. Wang, Q. Li, Y. W. Zhao, H. Hong, H. F. Li, Z. D. Huang, G. J. Liang, Q. Yang and C. Y. Zhi, Insight on Organic Molecules in Aqueous Zn-Ion Batteries with an Emphasis on the Zn Anode Regulation, *Adv. Energy Mater.*, 2022, **12**, 2102707.

54 J. Gao, X. Xie, S. Liang, B. Lu and J. Zhou, Inorganic Colloidal Electrolyte for Highly Robust Zinc-Ion Batteries, *Nano-Micro Lett.*, 2021, **13**, 69.

55 C. Guo, J. Zhou, Y. Chen, H. Zhuang, Q. Li, J. Li, X. Tian, Y. Zhang, X. Yao, Y. Chen, S. L. Li and Y. Q. Lan, Synergistic Manipulation of Hydrogen Evolution and Zinc Ion Flux in Metal-Covalent Organic Frameworks for Dendrite-free Zn-based Aqueous Batteries, *Angew. Chem., Int. Ed.*, 2022, **61**, e202210871.

56 J. H. Park, M. J. Kwak, C. Hwang, K. N. Kang, N. Liu, J. H. Jang and B. A. Grzybowski, Self-assembling films of covalent organic frameworks enable long-term, efficient cycling of zinc-ion batteries, *Adv. Mater.*, 2021, **33**, e2101726.

57 Z. M. Zhao, J. W. Zhao, Z. L. Hu, J. D. Li, J. J. Li, Y. J. Zhang, C. Wang and G. L. Cui, Long-life and deeply rechargeable aqueous Zn anodes enabled by a multifunctional brightener-inspired interphase, *Energy Environ. Sci.*, 2019, **12**, 1938–1949.

58 D. D. Wang, D. Lv, H. L. Peng, N. N. Wang, H. X. Liu, J. Yang and Y. T. Qian, Site-Selective Adsorption on  $ZnF_2/Ag$  Coated Zn for Advanced Aqueous Zinc-Metal Batteries at Low Temperature, *Nano Lett.*, 2022, **22**, 1750–1758.

59 K. Chen, H. Guo, W. Li and Y. Wang, Dual Porous 3D Zinc Anodes toward Dendrite-Free and Long Cycle Life Zinc-Ion Batteries, *ACS Appl. Mater. Interfaces*, 2021, **13**, 54990–54996.

60 J. Zheng, Q. Zhao, T. Tang, J. Yin, C. D. Quilty, G. D. Renderos, X. Liu, Y. Deng, L. Wang, D. C. Bock, C. Jaye, D. Zhang, E. S. Takeuchi, K. J. Takeuchi, A. C. Marschilok and L. A. Archer, Reversible Epitaxial Electrodeposition of Metals in Battery Anodes, *Science*, 2019, **366**, 645–648.

61 C. Li, Z. T. Sun, T. Yang, L. H. Yu, N. Wei, Z. N. Tian, J. S. Cai, J. Z. Lv, Y. L. Shao, M. H. Rummeli, J. Y. Sun and Z. F. Liu, Directly Grown Vertical Graphene Carpets as Janus Separators toward Stabilized Zn Metal Anodes, *Adv. Mater.*, 2020, **32**, 2003425.

62 Z. Wang, L. Dong, W. Huang, H. Jia, Q. Zhao, Y. Wang, B. Fei and F. Pan, Simultaneously Regulating Uniform  $Zn^{2+}$  Flux and Electron Conduction by MOF/rGO Interlayers for High-Performance Zn Anodes, *Nano-Micro Lett.*, 2021, **13**, 73.

63 X. Zhang, J. Li, K. Qi, Y. Yang, D. Liu, T. Wang, S. Liang, B. Lu, Y. Zhu and J. Zhou, An Ion-Sieving Janus Separator toward Planar Electrodeposition for Deeply Rechargeable Zn-Metal Anodes, *Adv. Mater.*, 2022, **34**, e2205175.

64 Y. Tian, Y. An, C. Wei, B. Xi, S. Xiong, J. Feng and Y. Qian, Recent Advances and Perspectives of Zn-Metal Free “Rocking-Chair”-Type Zn-Ion Batteries, *Adv. Energy Mater.*, 2021, **11**, 2002529.

65 M. Liu, L. Yang, H. Liu, A. Amine and F. Pan, Artificial solid-electrolyte interface facilitating dendrite-free zinc metal anodes via nano-wetting effect, *ACS Appl. Mater. Interfaces*, 2019, **11**, 32046–32051.

66 X. Xu, Y. Xu, J. Zhang, Y. Zhong, Z. Li, H. Qiu, H. B. Wu, J. Wang, X. Wang, C. Gu and J. Tu, Quasi-Solid Electrolyte Interphase Boosting Charge and Mass Transfer for Dendrite-Free Zinc Battery, *Nano-Micro Lett.*, 2023, **15**, 56.

67 W. L. Xin, J. Xiao, J. W. Li, L. Zhang, H. L. Peng, Z. C. Yan and Z. Q. Zhu, Metal-organic frameworks with carboxyl functionalized channels as multifunctional ion-conductive interphase for highly reversible Zn anode, *Energy Storage Mater.*, 2023, **56**, 76–86.

68 E. Kim, I. Choi and K. W. Nam, Metal-organic framework for dendrite-free anodes in aqueous rechargeable zinc batteries, *Electrochim. Acta*, 2022, **425**, 140648.

69 R. Zhang, Y. Feng, Y. Ni, B. Zhong, M. Peng, T. Sun, S. Chen, H. Wang, Z. Tao and K. Zhang, Bifunctional Interphase with Target-Distributed Desolvation Sites and

Directionally Depositional Ion Flux for Sustainable Zinc Anode, *Angew. Chem., Int. Ed.*, 2023, **62**, e202304503.

70 H. Yang, Z. Chang, Y. Qiao, H. Deng, X. Mu, P. He and H. Zhou, Constructing a super-saturated electrolyte front surface for stable rechargeable aqueous zinc batteries, *Angew. Chem., Int. Ed.*, 2020, **59**, 9377–9381.

71 X. Pu, B. Jiang, X. Wang, W. Liu, L. Dong, F. Kang and C. Xu, High-Performance Aqueous Zinc-Ion Batteries Realized by MOF Materials, *Nano-Micro Lett.*, 2020, **12**, 152.

72 W. Liu, P. Guo, T. Y. Zhang, X. W. Ying, F. L. Zhou and X. Y. Zhang, Rational Electrode-Electrolyte Design for Long-Life Rechargeable Aqueous Zinc-Ion Batteries, *J. Phys. Chem. C*, 2022, **126**, 1264–1270.

73 X. Liu, F. Yang, W. Xu, Y. Zeng, J. He and X. Lu, Zeolitic imidazolate frameworks as  $Zn^{2+}$  modulation layers to enable dendrite-free Zn anodes, *Adv. Sci.*, 2020, **7**, 2002173.

74 W. He, T. Gu, X. Xu, S. Zuo, J. Shen, J. Liu and M. Zhu, Uniform In Situ Grown ZIF-L Layer for Suppressing Hydrogen Evolution and Homogenizing Zn Deposition in Aqueous Zn-Ion Batteries, *ACS Appl. Mater. Interfaces*, 2022, **14**, 40031–40042.

75 X. Zeng, J. Zhao, Z. Wan, W. Jiang, M. Ling, L. Yan and C. Liang, Controllably Electrodepositing ZIF-8 Protective Layer for Highly Reversible Zinc Anode with Ultralong Lifespan, *J. Phys. Chem. Lett.*, 2021, **12**, 9055–9059.

76 X. Luo, Q. S. Nian, Z. H. Wang, B. Q. Xiong, S. Q. Chen, Y. C. Li and X. D. Ren, Building a seamless water-sieving MOF-based interphase for highly reversible Zn metal anodes, *Chem. Eng. J.*, 2023, **455**, 140510.

77 Y. Wang, Y. N. Liu, H. Q. Wang, S. M. Dou, W. Gan, L. J. Ci, Y. Huang and Q. H. Yuan, MOF-based ionic sieve interphase for regulated  $Zn^{2+}$  flux toward dendrite-free aqueous zinc-ion batteries, *J. Mater. Chem. A*, 2022, **10**, 4366–4375.

78 Z. Q. Wang, H. G. Chen, H. S. Wang, W. Y. Huang, H. Y. Li and F. Pan, In Situ Growth of a Metal-Organic Framework-Based Solid Electrolyte Interphase for Highly Reversible Zn Anodes, *ACS Energy Lett.*, 2022, **7**, 4168–4176.

79 H. Sun, Y. Huyan, N. Li, D. Lei, H. Liu, W. Hua, C. Wei, F. Kang and J. G. Wang, A Seamless Metal-Organic Framework Interphase with Boosted  $Zn^{2+}$  Flux and Deposition Kinetics for Long-Living Rechargeable Zn Batteries, *Nano Lett.*, 2023, **23**, 1726–1734.

80 F. F. Wang, H. T. Lu, H. Li, J. Li, L. Wang, D. L. Han, J. C. Gao, C. N. Geng, C. J. Cui, Z. C. Zhang, Z. Weng, C. P. Yang, J. Lu, F. Y. Kang and Q. H. Yang, Demonstrating U-shaped zinc deposition with 2D metal-organic framework nanoarrays for dendrite-free zinc batteries, *Energy Storage Mater.*, 2022, **50**, 641–647.

81 T. Xin, Y. R. Wang, Q. J. Xu, J. X. Shang, X. C. Yuan, W. X. Song and J. Z. Liu, Forming an Amorphous ZnO Nanosheet Network by Confined Parasitic Reaction for Stabilizing Zn Anodes and Reducing Water Activity, *ACS Appl. Energy Mater.*, 2022, **5**, 2290–2299.

82 D. D. Zhang, Y. Q. Fu, Q. L. Wei, Y. P. Zheng, L. Wang, J. Teng and W. Y. Yang, Controllable and large-area growth of ZnO nanosheet arrays under ambient condition as superior anodes for scalable aqueous batteries, *Carbon Energy*, 2023, e359.

83 J. Y. Kim, G. Liu, G. Y. Shim, H. Kim and J. K. Lee, Functionalized Zn@ZnO Hexagonal Pyramid Array for Dendrite-Free and Ultrastable Zinc Metal Anodes, *Adv. Funct. Mater.*, 2020, **30**, 2004210.

84 L. Cao, D. Li, T. Deng, Q. Li and C. Wang, Hydrophobic Organic-Electrolyte-Protected Zinc Anodes for Aqueous Zinc Batteries, *Angew. Chem., Int. Ed.*, 2020, **59**, 19292–19296.

85 J. Zhao, Y. P. Ying, G. L. Wang, K. D. Hu, Y. D. Yuan, H. L. Ye, Z. L. Liu, J. Y. Lee and D. Zhao, Covalent organic framework film protected zinc anode for highly stable rechargeable aqueous zinc-ion batteries, *Energy Storage Mater.*, 2022, **48**, 82–89.

86 C. Guo, J. Zhou, Y. Chen, H. Zhuang, J. Li, J. Huang, Y. Zhang, Y. Chen, S. L. Li and Y. Q. Lan, Integrated Micro Space Electrostatic Field in Aqueous Zn-Ion Battery: Scalable Electrospray Fabrication of Porous Crystalline Anode Coating, *Angew. Chem., Int. Ed.*, 2023, **62**, e202300125.

87 X. H. Hu, Z. Q. Lin, S. P. Wang, G. Y. Zhang, S. J. Lin, T. Huang, R. W. Chen, L. H. Chung and J. He, Highly Crystalline Flower-Like Covalent-Organic Frameworks Enable Highly Stable Zinc Metal Anodes, *ACS Appl. Energy Mater.*, 2022, **5**, 3715–3723.

88 V. Aupama, W. Kao-ian, J. Sangsawang, G. Mohan, S. Wannapaiboon, A. A. Mohamad, P. Pattananuwat, C. Sriprachuabwong, W.-R. Liu and S. Kheawhom, Stabilizing a zinc anode via a tunable covalent organic framework-based solid electrolyte interphase, *Nanoscale*, 2023, **15**, 9003–9013.

89 Z. Wang, J. H. Huang, Z. W. Guo, X. L. Dong, Y. Liu, Y. G. Wang and Y. Y. Xia, A Metal-Organic Framework Host for Highly Reversible Dendrite-free Zinc Metal Anodes, *Joule*, 2019, **3**, 1289–1300.

90 L. Lei, Y. Zheng, X. Zhang, Y. Su, X. Zhou, S. Wu and J. Shen, A ZIF-8 Host for Dendrite-Free Zinc Anodes and N, O Dual-doped Carbon Cathodes for High-Performance Zinc-Ion Hybrid Capacitors, *Chem.- Asian J.*, 2021, **16**, 2146–2153.

91 Y. Tao, S. W. Zuo, S. H. Xiao, P. X. Sun, N. W. Li, J. S. Chen, H. B. Zhang and L. Yu, Atomically Dispersed Cu in Zeolitic Imidazolate Framework Nanoflake Array for Dendrite-Free Zn Metal Anode, *Small*, 2022, **18**, e2203231.

92 Y. Song, P. Ruan, C. Mao, Y. Chang, L. Wang, L. Dai, P. Zhou, B. Lu, J. Zhou and Z. He, Metal-Organic Frameworks Functionalized Separators for Robust Aqueous Zinc-Ion Batteries, *Nano-Micro Lett.*, 2022, **14**, 218.

93 S. Naskar and M. Deepa,  $ZnV_2O_4$ -textured carbon composite contacting a ZIF-8 MOF layer for a high performance non-aqueous zinc-ion battery, *Batteries Supercaps*, 2022, **5**, e20210036.

94 Z. Q. Wang, J. T. Hu, L. Han, Z. J. Wang, H. B. Wang, Q. H. Zhao, J. J. Liu and F. Pan, A MOF-based single-ion  $Zn^{2+}$  solid electrolyte leading to dendrite-free rechargeable Zn batteries, *Nano Energy*, 2019, **56**, 92–99.

95 S. Park, I. Kristanto, G. Y. Jung, D. B. Ahn, K. Jeong, S. K. Kwak and S. Y. Lee, A single-ion conducting covalent organic framework for aqueous rechargeable Zn-ion batteries, *Chem. Sci.*, 2020, **11**, 11692–11698.

96 X. Gong, J. Wang, Y. Shi, Q. Zhang, W. Liu, S. Wang, J. Tian and G. Wang, Inhibiting dendrites on Zn anode by ZIF-8 as solid electrolyte additive for aqueous zinc ion battery, *Colloids Surf., A*, 2023, **656**, 130255.

97 S. Chen, Y. Ying, L. Ma, D. Zhu, H. Huang, L. Song and C. Zhi, An asymmetric electrolyte to simultaneously meet contradictory requirements of anode and cathode, *Nat. Commun.*, 2023, **14**, 2925.